International Journal of Nanomedicine

Dovepress
open access to scientific and medical research

Open Access Full Text Article

REVIEW

Antibiotic Nanoparticles-Loaded Wound Dressings Against *Pseudomonas aeruginosa*'s Skin Infection: A Systematic Review

María I Quiñones-Vico[1–4,*], Ana Ubago-Rodríguez[1–3,*], Ana Fernández-González[1–3], Raquel Sanabria-de la Torre[2,5], Álvaro Sierra-Sánchez[1–3,5], Trinidad Montero-Vilchez[2,6], Manuel Sánchez-Díaz[2,6], José L Arias[2,7,8], Salvador Arias-Santiago[1–4,6]

[1]Cell Production and Tissue Engineering Unit, Virgen de las Nieves University Hospital, Granada, 18014, Spain; [2]Instituto de Investigación Biosanitaria Granada ibs.GRANADA, Granada, 18014, Spain; [3]Andalusian Network of Design and Translation of Advanced Therapies, Sevilla, 41092, Spain; [4]Medicine Department, School of Medicine, University of Granada, Granada, 18016, Spain; [5]Department of Biochemistry and Molecular Biology Ili and Immunology, School of Medicine, University of Granada, Granada, 18016, Spain; [6]Dermatology Department, Virgen de las Nieves University Hospital, Granada, 18014, Spain; [7]Department of Pharmacy and Pharmaceutical Technology, School of Pharmacy, University of Granada, Granada, 18071, Spain; [8]Institute of Biopathology and Regenerative Medicine (IBIMER), Center of Biomedical Research (CIBM), University of Granada, Granada, 18100, Spain

*These authors contributed equally to this work

Correspondence: Ana Fernández-González, Email ana.fernandez.gonzalez@juntadeandalucia.es

Abstract: *Pseudomonas aeruginosa* (*P. aeruginosa*) is a common nosocomial pathogen that can cause severe infections in critically ill patients. Due to its resistance to multiple drugs, it is challenging to treat, which can result in serious illness and death. Conventional treatments for infected wounds often involve the topical or systemic application of antibiotics, which can lead to systemic toxicity and the development of drug resistance. The combination of wound dressings that promote wound healing with nanoparticles (NPs) represents a revolutionary strategy for optimizing the safety and efficacy of antibiotics. This review assesses a systematic search to identify the latest approaches where the evaluation of wound dressings loaded with antibiotic NPs is conducted. The properties of NPs, the features of wound dressings, the antimicrobial activity and biocompatibility of the different strategies are analyzed. The results indicate that most research in this field is focused on dressings loaded with silver NPs (57.1%) or other inorganic materials (22.4%). Wound dressings loaded with polymeric NPs and carbon-based NPs represent 14.3% and 6.1% of the evaluated studies, respectively. Nevertheless, there are no clinical trials that have evaluated the efficacy of NPs-loaded wound dressings in patients. Further research is required to ensure the safety of these treatments and to translate the findings from the bench to the bedside.

Keywords: hydrogel, skin infection, wound dressing, P. aeruginosa, nanoparticles

Introduction

Pseudomonas aeruginosa (P. aeruginosa) is a human opportunistic pathogen and one of the most common nosocomial pathogens associated with life-threatening acute and chronic infections in critically ill or immunocompromised patients. These include ventilator-associated pneumonia, structural lung disease such as cystic fibrosis, bloodstream and urinary tract infections. Furthermore, it is known to cause serious infections in cutaneous wounds, chronic ulcers and burn patients with trauma.[1–4] It is a multi-drug resistant (MDR) Gram-negative bacillus that, along with *Enterococcus faecium, Staphylococcus aureus, Klebsiella pneumoniae, Acinetobacter baumannii* and *Enterobacter* species, is considered an "ESKAPE" pathogen. This classification serves to highlight the impact of this bacterium on hospital infections and its ability to evade the effect of antibacterial drugs.[4,5] Importantly, the World Health Organization (WHO) has classified this pathogen as critical, priority 1, due to the urgent necessity for the development of new antibiotics and treatment strategies.[5]

Received: 19 March 2024
Accepted: 7 July 2024
Published: 2 August 2024

Graphical Abstract

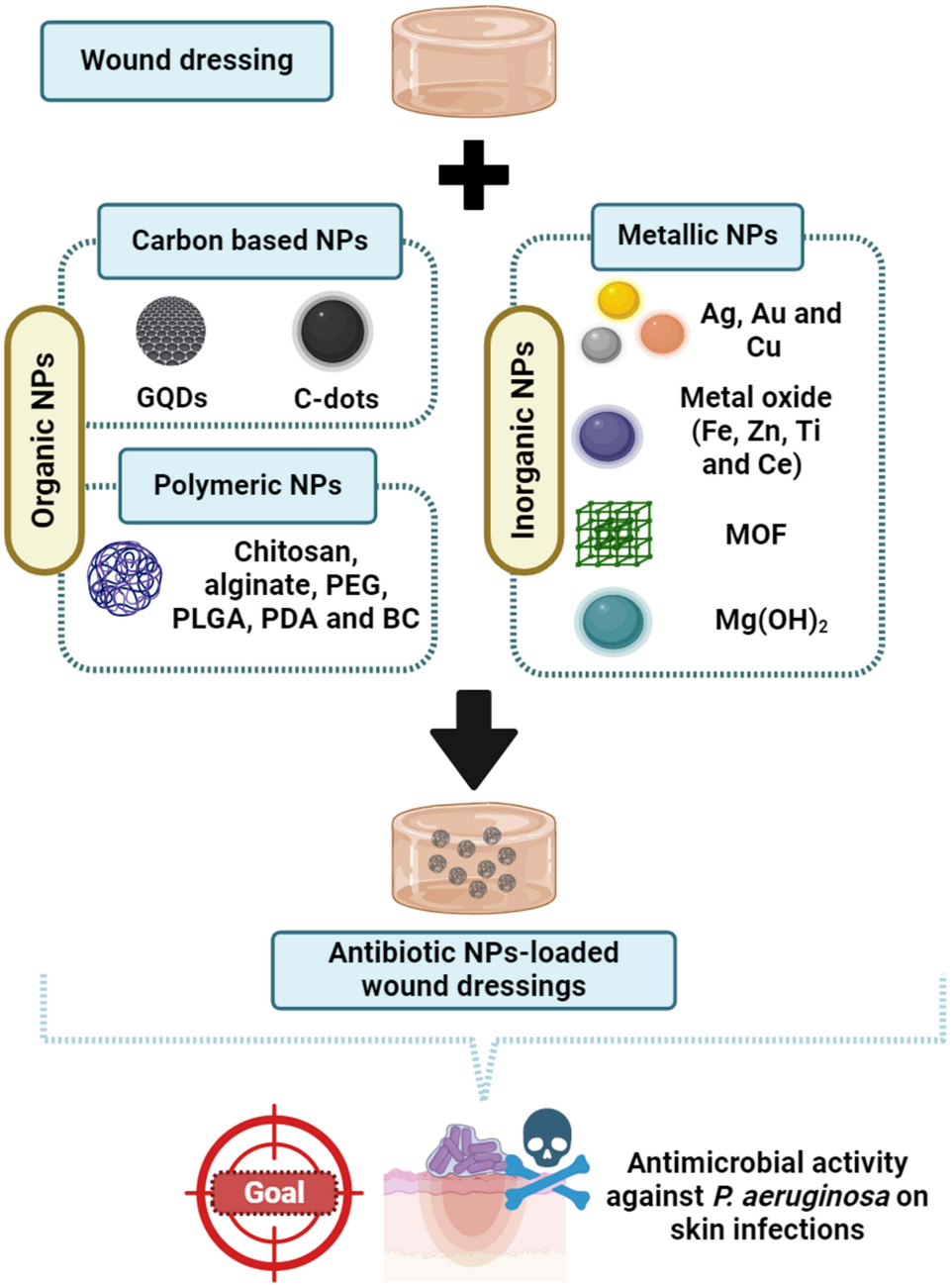

From an epidemiological perspective, it is estimated that *P. aeruginosa* has a prevalence of approximately 7.2% amongst all healthcare-associated infections, with notable morbidity and mortality associated with it.[6] Individuals with frequent or prolonged exposure to aqueous environments, diabetics, and immunocompromised patients are at high risk for developing *P. aeruginosa* skin infections.[7] Regarding skin infections, this bacterium is the most prevalent organism responsible for infection in burn-injured patients, associated with sepsis and mortality. MDR *P. aeruginosa* is becoming an increasingly common cause of death in these patients, with approximately 86% of sepsis deaths occurring in a pediatric burn intensive care unit.[6] Together with *Staphylococcus aureus*, it represents one of the most common agents

isolated from chronic leg ulcers, colonizing approximately 52.2% of patients. It is typically found in the deepest region of the wound bed.[8]

Biofilms, which are complex clusters of bacteria attached to a surface and embedded in a self-produced matrix, lead to the development of an organized microbial ecosystem in which *P. aeruginosa* develops antibiotic tolerance. The formation of biofilms is initiated by the attachment of a cell to a surface, subsequent multiplication, maturation, and the production of an extracellular polymeric matrix. This matrix serves to resist environmental impacts including mechanical forces and antibiotics.[9] Indeed, bacteria entrapped in biofilms can exhibit up to 1000-fold greater antibiotic tolerance than free-living bacteria.[2,10] In chronic wounds, *P. aeruginosa* exists as a polysaccharide-coated biofilm. The bacterial-derived polysaccharides facilitate bacterial survival, protection from the immune response, desiccation and oxidizing agents increasing the antibiotic resistance.[6]

In addition to the development of antibiotic tolerance, *P. aeruginosa* is intrinsically resistant to a number of antimicrobials due to the action of different mechanisms.[2,4,7] Briefly, the outer membrane permeability of this bacterium is reduced, which restrict the diffusion of antibiotics such as aminoglycosides and polymyxins through the cell envelope. Furthermore, these bacteria express multidrug efflux pumps which result in the exclusion of small hydrophilic antibiotics such as β-lactams and quinolones from the outer membrane through porins.[2] Finally, it produces antibiotic modification enzymes, such as chromosomal AmpC cephalosporinases. In fact, the hyperproduction of the chromosomal AmpC β-lactamase represents the primary mechanism responsible for β-lactam resistance in this bacterium.[11] Importantly, *P. aeruginosa* is capable of developing antibiotic resistance through chromosomal mutations, particularly those encoding metallo-β-lactamases or extended-spectrum β-lactamases, often co-transferred with genes encoding resistance to aminoglycosides and/or fluoroquinolones[3] and through horizontal gene acquisition.[2] Consequently, treatments for *P. aeruginosa* infection are extremely difficult due to its intrinsic resistance mechanisms, biofilm's tolerance development to antibiotics, and rapid mutations.

The conventional treatments for infected skin wounds are based on application of topical or systemic antibacterial compounds including antiseptics and antibiotics with the objective of overcoming the risk of bacterial resistance and reducing the systemic exposure to drugs.[12,13] In this context, wound dressings play an important role. Conventionally, they are used only to prevent external contamination of the wound. However, advances in this field have led to the development of advanced wound dressings that not only prevent bacterial infection but also combat it and promote wound healing. Thus, wound dressings can be functionalized with many classes of antibiotics or antibacterial compounds.[14] Such dressings allow the treatment of infected wounds that require high concentrations of antibiotics. However, the use of antibiotic-embedded wound dressings can result in the generation of systemic toxicity. Together with the emergence of bacterial resistance, this systemic toxicity determines the need for NPs- based advances.

NPs have demonstrated potent bactericidal effects on their own, when loaded with antibiotic or when used in combination. Thus, they can inhibit the growth of bacterial biofilms through physical damage, oxidative stress, thermal damage, and other specific mechanisms thereby enhancing the efficacy of antibacterial drugs and the overcoming of bacterial resistance caused by biofilms.[12,13,15] Due to their unique characteristics, including their small size, surface charge, and large specific surface area, NPs can gather in infection sites.[16] Moreover, depending on the design strategy employed, NPs can be engineered to release the drug in a controlled manner. This targeted approach enables the delivery of higher concentrations of therapeutic agents to cells and tissues, thus allowing for the use of lower doses. Moreover, by increasing the concentration of therapeutic agents in the target location, their effectiveness is enhanced making them more tolerable in biological systems.[17] Importantly, NPs should be biodegradable, non-toxic and non-immunogenic. These properties make them attractive to be included in wound dressings for the management of skin infections. This systematic review focuses on the latest advances in the wound dressings' development containing antibiotic NPs for the treatment of infected skin wounds caused by *P. aeruginosa*.

Characteristics of an Ideal Wound Dressing

It is evident that a considerable amount of blood is lost following an injury. Stopping this loss is often the first step in wound repair. Therefore, the dressing employed must possess a robust hemostatic capacity. This becomes a relevant factor in assessing the biocompatibility of dressings that come into direct contact with red blood cells.[18] In accordance with the American Society for Testing and Materials (ASTM F 756–00, 2000), the internationally safe hemolysis rate should be less than 5%.[19,20] In addition to being hemocompatible, the dressings must also be cytocompatible. In order for

a substance to be considered non-toxic in accordance with the ISO 2009 international standard for the biological evaluation of medical devices, the viability of the tested cell types must exceed 70%.[21]

During the initial stages of wound healing, wounds produce a considerable amount of exudate, particularly those resulting from burns. This excessive exudate presents a challenge as it impairs gas exchange, increasing the risk of wound infection.[22] Such infections can impede the repair and regeneration stages involved in the healing process, and even affect the restoration of anatomical and physiological integrity, leading to chronic wounds.[23] To eliminate this issue, dressings with a high absorption capacity, which can be assessed by the swelling ratio of the gel, are required to protect the wound from microbial contamination.[24,25]

At this level, it is important to consider a highly porous internal structure, with porosity ranging from approximately 60 to 90%.[26] This structure not only absorbs excess fluid but also allows for gas diffusion, thus enabling the wound to obtain nutrients and oxygen, creating an appropriate environment for cell growth.[24,27] The interconnected porous structure facilitates dermal fibroblast growth and migration, thereby promoting wound healing.[19] It also allows the loading of antibacterial drugs.[28]

However, although it may seem contradictory, it is essential to maintain a moist wound environment. The high-water content of the human body facilitates epidermal cell migration, angiogenesis, proliferation, collagen deposition, and re-epithelialization in an optimal aqueous environment.[24,27,29] In fact, Zhiyong et al[27] have investigated the potential of asymmetric materials, wherein one side would exhibit hydrophilic properties to absorb exudates, while the other would display hydrophobic characteristic to protect against airborne microorganisms, thereby reducing the risk of infection. In addition, it prevents evaporative water loss from inside the wound, maintaining the moist environment that would enhance wound healing. Therefore, wound dressings should regulate moisture loss and absorption to create an optimal moist environment that facilitates drug release.[28,30]

The Water Vapor Transmission Rate (WVTR) determines the capacity of wound dressings to regulate water loss during the healing process. Dressings with a WVTR value of 1800 −2200 $g \cdot m^{-2} \cdot 24\ h^{-1}$ are ideal for maintaining optimal moisture content. A higher value may result in scarring of the surface due to excessive dehydration, while lower values may lead to the formation of exudates on the wound surface, increasing the risk of bacterial contamination.[31]

The healing process can be affected by various factors, including high oxidative stress at the wound site caused by immune cells during inflammation. The release of high levels of reactive oxygen species (ROS) can trigger cell apoptosis, which can disrupt the healing process. As a result, there is a search for bandages with antioxidant properties to protect cells from damage.[23,32]

Regarding the mechanical properties of the wound dressing, rheology represents the most crucial technique for defining the characteristics of gels, which are essential for the creation of a robust scaffold.[33] Biomaterials with good strength and mechanical stability are preferred to reduce susceptibility to damage during application.[22,34] Additionally, materials with the ability to revert to their original shape (memory materials) have been studied. They can be compressed into a small volume, allowing for easy transportation and application to the wound using a syringe, without any deformation.[22,35] Accordingly, a reduction in viscosity at high shear rates and during storage is preferable for this type of material.[36] Several factors can affect the rheological properties, including the distribution of fibers within the material.[33,37]

Another important aspect is to maintain a pH within the range of the skin (6.0–7.0). Basic or acidic pHs could irritate the skin and affect the penetration of biomaterial components as well as their ability to adhere to the skin.[38]

Wound dressings should be biodegradable to avoid painful removal procedures for patients. If the compound used can be absorbed by the body, it would be expected to improve the patient's quality of life.[22] In this context, transparent dressings are preferred in order to allow for proper wound monitoring by clinicians. To prevent the disruption of granulation tissue and causing trauma to the wound,[23] it is recommended that the dressing be left in place until the wound has healed sufficiently. Traditional dressings can damage the granulation tissue and cause bleeding when changed, which can delay wound healing.[28] Therefore, it is important to find a dressing that is both cosmetically acceptable and cost-effective.[24]

Hydrogels used as wound dressings provide physical support and influence the survival of normal cells through interactions with cell membrane receptors. Consequently, the histological assessment will encompass the reduction of inflammatory cells, collagen deposition, and the appearance of new blood capillaries which facilitate the delivery of growth factors and nutrients to the damaged tissue.[39]

Finally, dressings are designed to have antimicrobial properties by incorporating compounds that can kill microorganisms, both individually and in biofilm formation. These compounds must not be eliminated by wound secretions such as blood, albumin, or pus.[24,30,40] This review will discuss the different alternatives.

Therefore, it is essential to develop a wound dressing with optimal hemostatic capacity, absorption, and adhesion, while maintaining wound moisture, high porosity, and superior physical properties (strength, stability, biodegradability, and transparency). The dressing should also be biocompatible, possess an appropriate pH, and exhibit antimicrobial properties to facilitate wound repair, enhance wound appearance, and reduce healing time (Figure 1). [25,35,41]

Materials and Methods

Search Strategy

This systematic review was conducted and reported according to the Preferred Reporting Items for Systematic Reviews and Meta-analyses (PRISMA) reporting guideline.[42] On December 27, 2023, a systematic bibliographic search was performed using MeSH and free-text terms at two distinct electronic databases: "Pubmed" and "Scopus". For this, a combination of terms was used in the search algorithm: the term "ANTIBIOTIC NANOPARTICLES" was combined using the boolean operator "and" with "PSEUDOMONAS AERUGINOSA" [Mesh] and with the following terms: "WOUND DRESSING", "ARTIFICIAL SKIN", "SKIN SUBSTITUTE" or "HYDROGEL". A total of 327 results were obtained.

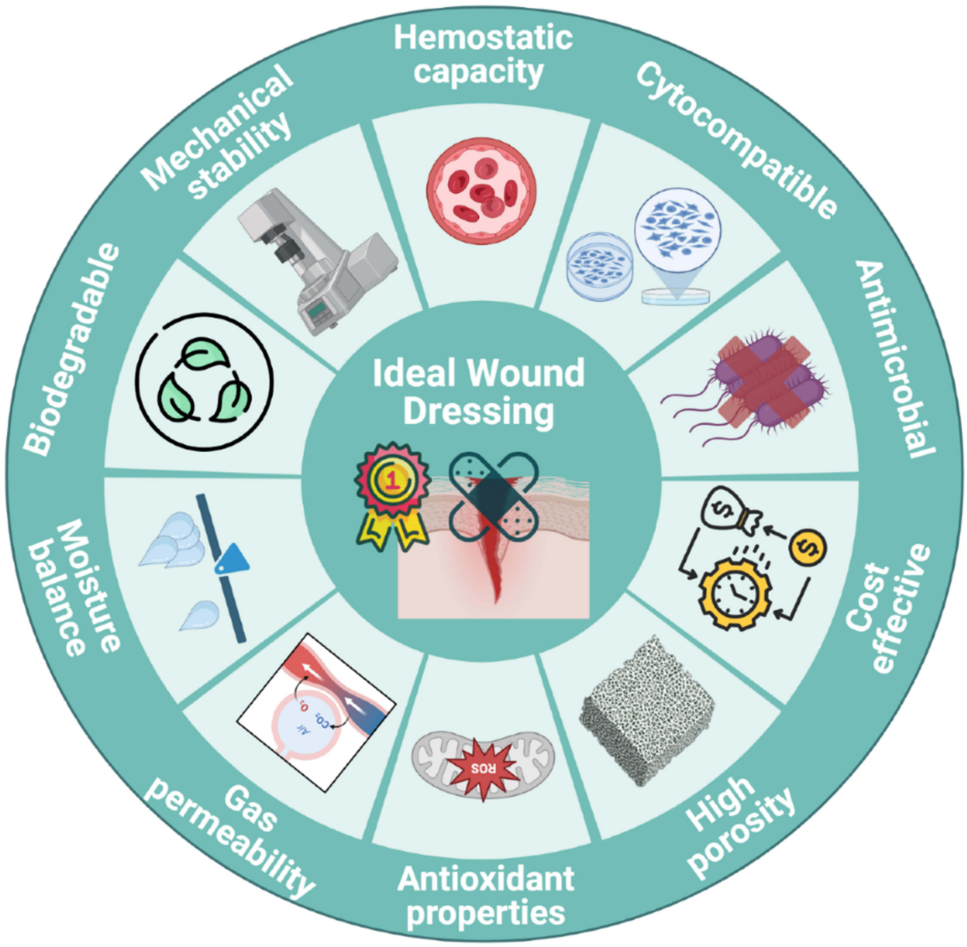

Figure 1 Characteristics of an ideal wound dressing. Mechanical stability, moisture balance, high porosity, gas permeability, hemostatic and antimicrobial capacity, cytocompatibility, biodegradability and cost-effectiveness are represented. Created with Biorender.com.

Eligibility Criteria

The inclusion criteria were: (1) wound dressing/artificial skin/skin substitute/hydrogel for skin infections, (2) loaded with antibiotic NPs, (3) with antimicrobial activity against *P. aeruginosa*, (4) where cytotoxicity of NPs was evaluated, (5) original article, (6) written in English language, (7) publications dated from January 2019 to December 2023. Exclusion criteria were: (1) non-research papers (books, reviews, letters to editor, protocols, clinical trials and unpublished literature), (2) non-skin infections and (3) articles where the antimicrobial capacity against *P. aeruginosa* was not evaluated. Finally, a total of 49 original research studies about wound dressing containing antibiotic NPs with antimicrobial activity against *P. aeruginosa* were included (Figure 2).

Study Selection

After date restriction and removal of duplicates, unpublished literature, clinical trials, protocols, letters to editor, books and reviews, search results were screened by two independent authors (MI.Q.V and A.U.R) based on title and abstract. References not meeting the inclusion criteria were excluded. After that, candidate articles were full text read autonomously by the same two authors ensuring that they fulfilled the rest of inclusion criteria. Any discrepancies about inclusion or exclusion of articles were discussed and resolved by a third independent reviewer (A.F.G).

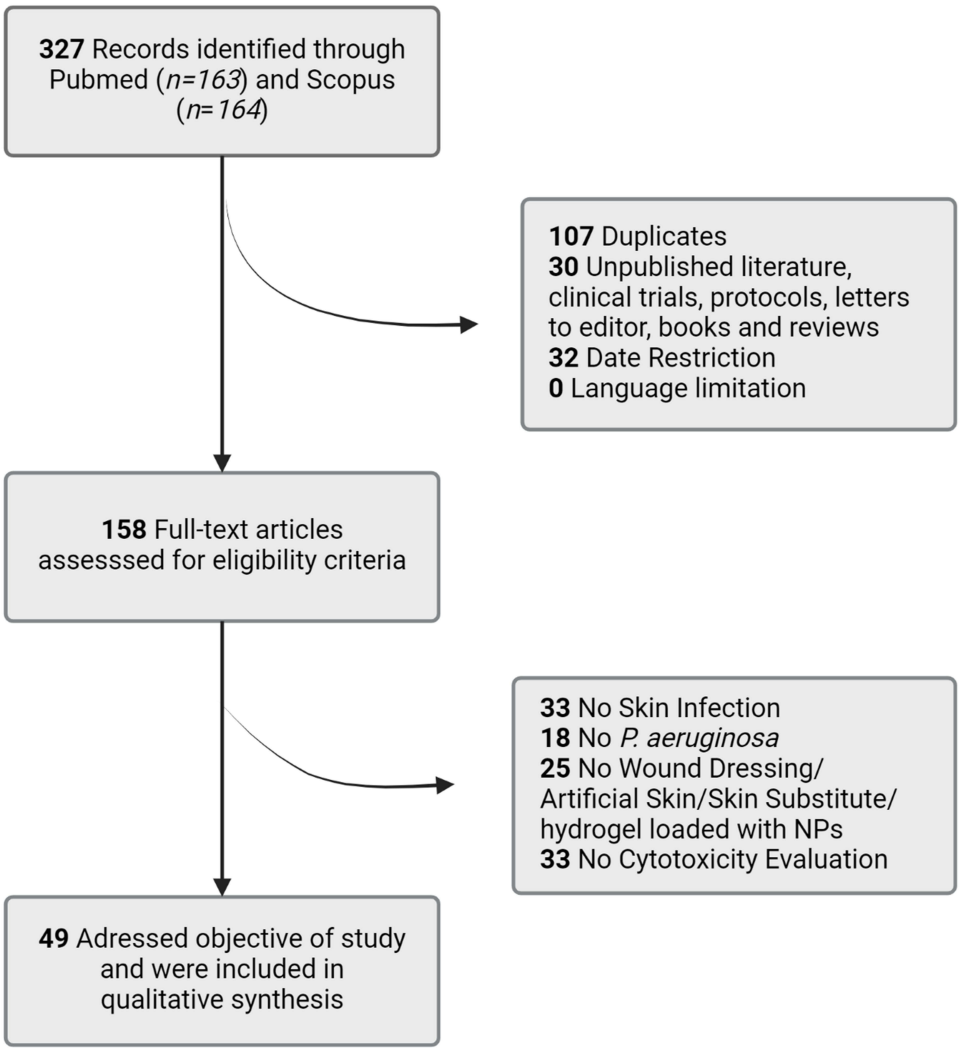

Figure 2 Procedure to select studies for inclusion in the systematic review following PRISMA guidelines. From 327 records identified, 158 full-text articles were assessed for eligibility criteria after date restriction and removal of duplicates, unpublished literature, clinical trials, protocols, letters to editor, books and reviews. Finally, 49 results met the inclusion criteria and were included in the qualitative analysis. Created with Biorender.com.

Results

Organic NPs Loaded Wound Dressings

Carbon Based NPs Loaded Wound Dressings

This systematic review identified two different approaches of wound dressings loaded with carbon-based NPs: graphene quantum dots (GQD) and carbon dots (C-dots). Table 1 presents the composition of the wound dressing, the antimicrobial agent, the properties of NPs, the properties of the wound dressing, the antimicrobial efficacy and the biocompatibility of each approach. Specifically, three studies have been found in this search.

GQD-based wound dressings have demonstrated several properties of an ideal wound dressing including good wound fluid absorption, water retention and hemostatic capacity, a porous network structure and self-healing ability, among others.[43,44] Furthermore, Cheng et al demonstrated that the dressing exhibited a photothermal effect following xenon light (XL) irradiation, resulting in a pronounced antibacterial efficacy.[44] In addition to being biocompatible to human fibroblasts (HFs), these GQDs-based dressings have been demonstrated to promote angiogenesis and accelerate wound healing in infected diabetic mice.[43,44] Carbon-based NPs-loaded into wound dressings are also capable of suppressing bacterial proliferation by removing Fe^{3+} ions from the environment. This exemplified by C-dot-loaded dressings, which are also biocompatible and capable of being 3D bioprinted as wound patches.[45]

With regard to antimicrobial activity, Zmejkoski et al[43] observed the absence of bacterial growth on plates, although no quantified data were provided. Cheng et al[44] reported almost zero growth on plates and observed pores in the bacterial membrane under microscopy. Chekini et al[45] evaluated the reduction of bacterial colonies grown on plates and obtained a value of approximately 66%.

Polymeric NPs Loaded Wound Dressings

Polymeric NPs loaded in wound dressings are composed of poly(lactic-co-glycolic) acid (PLGA), alginate, chitosan, polydopamine (PDA) and bacterial cellulose (BC). Table 2 provides a summary of the eight approaches of polymeric NPs that have been developed to date to deliver antimicrobial agents to the wound site through wound dressings.

Ciprofloxacin (CIP), cefepime and polymyxin B were the delivered antimicrobial agents by polymeric NPs. Particularly, CIP was encapsulated by PDA[50] and PLGA NPs.[52] Sodium alginate NPs were used for the encapsulation of polymyxin B[51] while chitosan NPs were employed for the encapsulation of cefepime.[47] Three studies evaluated wound dressings containing empty NPs made of PDA[46] and a combination of BC and chitosan.[48,49] All these studies showed antibacterial efficacy against *P. aeruginosa*.

Regarding the cytotoxic impact of these wound dressings, those loaded with PDA NPs exhibited biocompatibility with a range of cell lines in vitro, including human lung embryonic cells (MRC-5),[46] mouse embryonic osteoblasts (MC3T3-E1)[46] and HFs.[50] They also demonstrated complete wound healing in vivo.[46] Chitosan NP-loaded dressings were found to be biocompatible with HT1080[47] and human gingival cells (HGCs).[48,49] As PDA NPs, they showed 100% of wound closure in vivo.[47] Wound dressings incorporating alginate NPs exhibited biocompatibility in vivo promoting wound healing. However, they reduced L929 cell viability in vitro after 24 hours of exposure.[51] PLGA NPs-loaded dressing showed no cytotoxicity to human mesenchymal stem cells (hMSCs) and HaCaTs in vitro but in vivo biocompatibility was not evaluated.[52]

All these dressings presented essential properties, including adequate mechanical strength, thermal stability, water retention and absorption and flexibility. Zhe et al also reported the extrudability and self-healing capacity of their wound dressing, which incorporated chitosan NPs.[46] Similarly, Zmejkoski et al reported the use of chitosan NPs in a similar dressing type. In this case, the dressing exhibited antioxidant properties, although the porosity was relatively low (up to 2.4%).[48,49]

As with other NPs groups, a variety of assay methods have been used to evaluate antimicrobial activity. Three papers assessed the agar disk diffusion assay,[47,51,52] with inhibition zones ranging from 19 mm[51] to 40 mm.[52] One paper examined optical density measurements through turbidity tests,[50] while another used the bacteria killing assay.[46] Only one paper evaluated the minimum inhibitory concentration (MIC), defined as the lowest concentration at which a material exhibits antimicrobial activity through serial dilution.[51] Only two articles reported on the ability of experimental dressings to damage bacterial biofilms.[48,49]

Inorganic NPs Loaded Wound Dressings

Metal NPs are a typical example of this class. They are composed exclusively of metal precursors and can be monometallic, bimetallic or polymetallic. All articles on the use of inorganic NPs found during the search are listed in Table 3.

Table 1 Carbon Based NPs-Loaded Wound Dressings Against *P. aeruginosa* Skin Infection

Wound dressing	Antimicrobial agent	NPs properties	Most Significative Wound Dressing Properties	Antimicrobial efficacy	Biocompatibility	Ref.
BC impregnated GQDs.	GQDs.	Diameter: 10 ± 2 nm. Height: 1.8 nm.	Anomalous or non-fickian diffusion release. Good wound fluid absorption and water retention.	Inhibitory and bactericidal effects. No values determined.	Did not affect HFs viability and migration. Promoted angiogenesis.	[43]
Quaternized chitosan, ε-PL grafted GQDs and benzaldehyde terminated 4 arm PEG hydrogel.	GQDs-ε-PL.	Size: 53 nm. Photothermal effect after XL irradiation.	In situ and spray gelation. Porous network structure. Almost transparent. Good photothermal performance and ability to repeatedly stimulate the photothermal conversion. pH-dependent degradation. Self-healing ability and good hemostatic capacity.	2% of bacterial viability after XL treatment.	Promoted NIH3T3 migration and proliferation, enhanced platelet endothelial cell adhesion and accelerated infected diabetic wound healing.	[44]
Nanocolloidal hydrogel based on CNCs decorated with C-dots.	C-dots.	Diameter: 1.6 ± 0.9 nm.	Fibrillar structure: 31 ± 11 nm fibril diameter. High degree of Fe^{3+} ion sequestration from the liquid environment. Capability of being 3D bioprinted as wound patches.	Reduction of the number of bacteria CFU: 66%.	Non cytotoxic to HF.	[45]

Abbreviations: BC: bacterial cellulose; C60: carbon 60; C-dots: carbon dots; CFU: colony-forming units; CNCs: cellulose nanocrystals; GQDs: graphene quantum dots; HFs: human fibroblasts; NIH3T3: fibroblasts from a mouse NIH/Swiss embryo; NPs: Nanoparticles; PEG: poly(ethylene glycol); PL: poly-L-lysine; Ref: reference; XL: xenon light.

Table 2 Polymeric NPs-Loaded Wound Dressings Against *P. aeruginosa* Skin Infection

Wound dressing	Antimicrobial agent	NPs properties	Most Significative Wound Dressing Properties	Antimicrobial efficacy	Biocompatibility	Ref.
Gelatin-based hydrogel containing SC-PDA NPs.	SC-PDA NPs.	ND.	Extrudable and self-healing capacity. Strength and thermal stability. Strong wet adhesion. Photothermal agent.	Almost 100% antibacterial activity after 6h of exposure.	Non cytotoxic to MRC-5 cells and MC3T3-E1. Non-immunogenic. Good hemocompatibility. Complete and accelerated healing in vivo.	[46]
Hydrogel membrane based on HA, pullulan and polyvinyl alcohol and loaded with chitosan based cefepime NPs.	Cefepime.	Size: 172 nm. Zeta potential: +27.8mV. Release: 88% in a sustained manner for 24h.	Smooth surface. Uniform thickness, flexibility and mechanical strength. Thermal stability. Optimal WVTR. Oxygen permeability.	Inhibition zone: 19 mm.	No cytotoxic to HT1080 cells. 100% wound closure at day 14 in vivo.	[47]
nChiD encapsulated in a BC polymer matrix.	nChiD	Size: 48–52 nm. Release: continuous in small amount (5–20%) during 72h.	Fibrous structure. Up to 2.4% porosity. Good water absorption. performance. Water retention for 5–7 hours. Moderate antioxidant ability.	Reduction of viable pathogenic bacteria in biofilm: 88%. Biofilm height reduction: up to 40%.	Non cytotoxic to HGCs. Positive effect on cell migration.	[48,49]
Gellan gum/PDA based hydrogels loaded with CIP.	CIP.	ND.	High water absorption. High hydrolytic resistance under physiological conditions. PDA dose dependent photothermal effect. CIP is released gradually.	Complete sterilization after photothermal treatment.	Non cytotoxic to HFs.	[50]

(*Continued*)

https://doi.org/10.2147/IJN.S469724

Table 2 (Continued).

Wound dressing	Antimicrobial agent	NPs properties	Most Significative Wound Dressing Properties	Antimicrobial efficacy	Biocompatibility	Ref.
Double layer biomembrane: chitosan, hydroxypropyl methylcellulose and lidocaine chloride in the first layer, and of sodium alginate-polymyxin B sulphate NPs as the second layer.	Polymyxin B.	ND.	Excellent thickness and adequate mechanical properties. Compatible pH for lesion application.	MIC: 144.5 μg/mL. Halo size growth inhibition (not quantified).	Reduced cell viability percentage of L929 cells after 24 h of incubation. Correct healing process in vivo. Satisfactory WRI at days 14 and 21.	[51]
CIP-loaded PLGA NPs incorporated electrospun fibers.	CIP.	Size: 108–226 nm. Zeta potential: −30.5 to −30.8 mV. EE: 60.7–74.1%. Release: Fick's diffusion followed by polymer-driven release (~60% in 24h).	ND.	Inhibition zone: 40 mm. NPs were able to hamper bacterial adhesion and invasiveness on HaCaTs.	No cytotoxic effects on hMSCs and HaCaTs.	[52]

Abbreviations: BC, bacterial cellulose; CIP, ciprofloxacin; EE, entrapment efficacy; HA, hyaluronic acid; HaCaTs, human immortalized keratinocyte cell line; HFs, human fibroblasts; HGCs, human gingival cells; hMSCs, human mesenchymal stem cells; HT1080 cells, epithelial cells derived from connective tissue from a patient with Fibrosarcoma; L929 cells, mouse fibroblast cell line; MC3T3-E1, mouse embryonic osteoblasts; MCRC-5 cells, human lung embryonic cells; MIC, minimum inhibitory concentration; nChiD, nanochitosan dots; ND, not determined; NPs, nanoparticles; PDA, polydopamine; PLGA, poly(lactic-co-glycolic) acid; Ref, reference; SC, self-assembly confined; SF, silk fibroin; WRI, wound refraction index; WVTR, water vapor transmission rate.

Table 3 Inorganic NPs-Loaded Wound Dressings Against *P. aeruginosa* Skin Infection

Wound Dressing	Antimicrobial Agent	NPs Properties	Most Significative Wound Dressing Properties	Antimicrobial Efficacy	Biocompatibility	Ref.
Chitosan/poloxamer 407 hydrogel loaded with AgNPs.	AgNPs.	Size: 76.12 nm. Zeta potential: −29 mV.	Homogeneous distribution of AgNPs. Water retention (85%). Porous structure. Rapid gelation under physiological conditions.	MIC: 8 μg/mL. MBC: 32 μg/mL.	Not cytotoxic to THP-1 macrophages.	[53]
3D-printed collagen-HA hydrogel loaded with AgNCs.	AgNCs.	Size: 3–7 nm. Zeta potential: −29 mV.	High porosity (~60%). Moisture retention ability. Good mechanical properties. Good shear-thinning performance. Extrudable and suitable for bioprinting.	Inhibition zone: 15 mm.	Not cytotoxic to NIH3T3 cells. Promoted cell migration after 24 h. Accelerated wound healing, promoted collagen regeneration and deposition and reduced inflammation in vivo.	[54]
BC-HA hydrogel loaded with AgNPs.	AgNPs.	Size: 57.88 nm.	Dense network with few empty spaces and presence of pores.	MIC: 1.5 μg/mL. Time-kill assay: 99.99% of bactericidal efficacy after 3h exposure to the hydrogel.	Good hemocompatibility.	[55]
3D-printed AgNPs and TiO_2-embedded chitosan or sodium alginate hydrogels.	AgNPs.	ND.	Homogeneous distribution of AgNPs. Water content (>87%). High mechanical strength but low elasticity in alginate hydrogels.	Inhibition zone: 6 mm. TiO_2 did not show synergic effects.	Not cytotoxic to HFs. Chitosan showed higher biocompatibility. TiO_2 did not affect viability.	[56]
Sodium alginate/chitosan composite sponge containing Cur-loaded Se-synthesized AgNPs.	Cur-Se-AgNPs.	Size: 5–20 nm. Well-dispersed in solution.	Moisture retention ability. Ser increased hydrophilicity and swelling. High porosity (67.32%). Good mechanical properties.	Bacterial kill ratio: 81.33%. Bacterial cell viability: 20%.	Not cytotoxic to HUVECs and HaCaTs after 24 h. Good hemocompatibility. Promoted epithelial regeneration and collagen deposition in vivo. Stimulated angiogenesis while reducing inflammation in vivo.	[19]

(*Continued*)

https://doi.org/10.2147/IJN.S469724

Table 3 (Continued).

Wound Dressing	Antimicrobial Agent	NPs Properties	Most Significative Wound Dressing Properties	Antimicrobial Efficacy	Biocompatibility	Ref.
Chitosan and carrageenan hydrogel loaded with AgNPs and/or CuNPs.	AgNPs and/or CuNPs.	ND.	Lower porosity after incorporating NPs (ND). NPs provide higher thermal stability. Antioxidant capacity. Swelling (< 400%).	Inhibition zone of 10 mm (AgNPs), 16 mm (CuNPs) and 15 mm (Ag-CuNPs).	Only CuNPs-loaded hydrogel showed Vero cell viability above 70%.	[57]
Chitosan hydrogel with C_3N_4, PDA and AgNPs.	AgNPs. + C_3N_4 (visible light irradiation).	ND.	Tensile strength, elongation at break and good swelling rate. Rapid release of Ag^+ in the first 5 days (~6%) and a slow-release trend (~8%) for 15 days.	High antibacterial rate after 24 h. Photocatalytic antibacterial activity: >80%. After treatment, the bacteria membrane is broken.	Non cytotoxic to L929 cells. Cells retained their original spindle-shaped morphology. Good hemocompatibility. Did not cause pathological in vivo alterations. Promoted in vivo wound healing by facilitating collagen deposition and accelerating epidermal regeneration.	[34]
Sponge composed of sodium alginate-chitosan embedded with AgNPs synthesized with Se and loaded with Cur.	AgNPs. + Cur.	Size: 5–20 nm.	Excellent hygroscopicity, moisture retention ability, 67.3% porosity and mechanical properties. Stable for 2 days.	Bacterial kill ratio: 81.33%.	Non cytotoxic to HaCaTs and HUVECs. Good hemocompatibility. Promoted in vivo epithelial regeneration and collagen deposition with orderly distribution in infected wounds. Promoted in vivo angiogenesis and reduced inflammation.	[19]
Polyethylene mesh loaded with AgNPs (Acticoat™) + different coating formulations (chlorhexidine).	AgNPs. + chlorhexidine.	ND.	Uniform distribution of NPs.	Bacterial growth was seen on Acticoat alone but not on coated dressings.	Acticoat™ may be cytotoxic after 24 h and this increased when used with coating formulations on hKT. Cornified epidermal layer was absent from all samples overlaid with Acticoat™ for 72 h.	[58]

Guanidinium-hydrazide(AD-L)–Ag(0) NPs (AD-L@Ag(0)) hybrid gel.	Ag(0). + guanidinium ions.	Size: 5 nm. Zeta Potential: +30 mV. Stable for more than 6 months when stored in the gel matrix at ~10 °C.	Light orange colour. Linear viscoelastic behavior. Entangled fibril morphology. AgNPs uniformly distributed.	MIC and MBC: 0.78 μg/mL. $MBIC_{50}$: 3.125 μg/mL. $MBIC_{90}$: 1.56 μg/mL. Extensive damage of the biofilm membrane.	Non cytotoxic to Vero-E6 cell line.	[33]
PVA-HPMC with AgNPs hydrogel.	AgNPs.	Size:12–80 nm. Zeta Potential: -35 mV.	Enhanced haemostasis. Good antioxidant activity. Did not alter natural water loss from the body surface. Porosity (15%), moisture content (10%) and swelling (350%). Surface pH within the range of skin pH. High elasticity and folding endurance values. High stability and water vapor permeability.	Decreased the growth with >3 log (99.9%) following the treatments for 1 h.	Non cytotoxic to HaCaTs, L929 and RAW 264.7 cell lines. Promoted proliferation and migration of HaCaTs. Accelerated the in vivo wound healing and tissue regeneration process.	[38]
Electrospun chitosan NFs containing AgNPs loaded with Cur.	AgNPs. + Cur. + Chitosan.	Size: ~60 nm. Zeta potential: −31 mV. Excellent stability. Fast release of Cur in 48h (~60%, pH 5.5).	Smooth surface of NFs. High water absorption capability, adhesion and biodegradability.	Halo size growth inhibition (not quantified).	Non cytotoxic to L929 cells. Good hemocompatibility. Accelerated in vivo wound healing with less scar formation. Induced earlier granulation tissue formation, decreased number of inflammatory cells and displayed earlier epithelialization and thicker epidermis.	[20]

(*Continued*)

https://doi.org/10.2147/IJN.S469724

Table 3 (Continued).

Wound Dressing	Antimicrobial Agent	NPs Properties	Most Significative Wound Dressing Properties	Antimicrobial Efficacy	Biocompatibility	Ref.
Thermosensitive hydrogel based on poloxamers loaded with biosynthesized AgNPs.	AgNPs.	Shape: spherical.	Strong antioxidant capacity. Shear-thinning behavior. Dense 3D porous structure and rough surface. AgNPs uniformly distributed. Good mucoadhesive performance. AgNPs continuous release: zero-order profile. Stable during freeze and thaw cycles.	MIC:1.09 μg/mL. MBC: 17.5 μg/mL. Inhibited biofilm formation and eradicated cell viability within mature biofilms in a concentration-dependent manner.	Non cytotoxic to RAW 264.7 cell line. Anti-inflammatory effect.	[32]
PVA-GA-PCL NFs coated with LAB - green Fe_2O_3 NPs.	Fe_2O_3 NPs-LAB.	Size: 61.7 ± 30 nm.	Smooth and continuous surfaces.	Inhibition zone: 17 ± 0.57 mm. MIC: 37.5 μg/mL. MBC: 150 μg/mL. Biofilm inhibition: 43.73%.	Non cytotoxic to MEF cell line.	[59]
Hydrogel nanocomposite based on modified gelatin and iron-metal-organic framework and loaded with CS.	CS (antibacterial herbal drug).	500 nm (MIL-53 (Fe) NPs).	Slow and non-explosive release of CS. High thermal stability and water retention ability. Stable 3D lattice structure and good mechanical strength. Lattice state, greater porosity and high-water absorption.	Inhibition zone: 22 ± 4 mm. MIC and MBC: 6.25 ± 1 μg/mL	Non cytotoxic to HFF cell lines.	[60]
Gelatin cryogel loaded with AgNPs.	AgNPs.	Size: 10–20 nm.	Good mechanical strength and stability. High swelling ratio. Shape memory behavior. Interpenetrating porous structure. Good biodegradability.	Outstanding antibacterial ability (ND values). Biofilm Inhibition: 70%.	Non cytotoxic to L929 cells. Good hemocompatibility and hemostasis. Accelerated in vivo wound closure and promoted collagen deposition. Reduced inflammatory cells and stimulated angiogenesis.	[22]

Oxidized dextran and adipic dihydrazide grafted HACC and AgNPs hydrogel.	AgNPs. + HACC.	Size: 60–190 nm.	Good porosity (72.6%). Suitable swelling property, stable rheological behavior and suitable degradation rate.	Inhibition zone: 27 mm.	Non cytotoxic to L929 cells. Accelerated in vivo wound closure with small scar after healing at day 21. Almost complete re-epithelialization and well-organized collagen deposition. Anti-inflammatory effect.	[26]
Cotton fabric impregnated with SNPNPs.	SNPNPs.	Size: 30 ± 8 nm.	Long-term durability. Uniformly dispersed on the cotton surface Hydrophobic dressing.	Inhibition zone: 15 mm.	Promoted migration of in vitro endothelial cells. No obstruction in the formation of in vivo blood vessels. Absence of Ag ions from the vital organs. Enhanced in vivo wound healing. Increased re-epithelialization and deposition of connective tissue.	[24]
Dynamic hydrogel based on phenylboronic acid-modified HA and polyphenol-tannic acid loaded with AgNPs.	AgNPs.	Size: 10–35 nm.	pH and ROS dual stimuli responsiveness for drug delivery. Antioxidant ability. Brown color and microporous structures. Elasticity, injectability and self-healing properties.	Inhibition zone: 14 mm. MIC: 2.0 μg/mL.	Non cytotoxic to L929 cells. Good hemocompatibility.	[18]
Sodium alginate hydrogels loaded with AgNPs.	AgNPs.	Size: 350–450 nm. Zeta potential: −30 to −50 mV.	Homogeneous distribution of NPs.	MIC: 0.298 ± 0.02 μg/mL.	Non cytotoxic to L929 cells.	[61]
Chitosan hydrogel loaded with AgNPs and calcium alginate NPs.	AgNPs.	Size: 20–35 nm. Zeta potential: −35.4 ± 0.9 mV. Highly stable nature. Spherical shape.	Elastic, biodegradable, spreadable and easy to apply. Long term stability. Release of AgNPs in a continuous and sustained manner.	Inhibition zone: 9.2 ± 0.3 mm.	Accelerated in vivo wound healing with less scar formation and few inflammatory cells. Uniform and regular distribution of collagen bundles with reconstruction of new blood vessels.	[62]

(*Continued*)

https://doi.org/10.2147/IJN.S469724

Table 3 (Continued).

Wound Dressing	Antimicrobial Agent	NPs Properties	Most Significative Wound Dressing Properties	Antimicrobial Efficacy	Biocompatibility	Ref.
GA-PVA-PCL NFs matrix containing LAB-ZnONPs.	LAB-ZnONPs.	Size: 128 nm. Zeta potential: −15.03 mV.	NFs are long and continuous without beads.	Inhibition zone: 24 ± 0.57 mm. MIC: 18.75 μg/mL. MBC: 37.5 μg/mL. Biofilm inhibition: 49.65 ± 8.76%	Non cytotoxic to MEF cell line.	[63]
Chitosan/polyethylene oxide NFs armed with AgNPs and ZnONPs.	AgNPs and ZnONPs.	ND.	Improved nanofibrous mats' tensile properties and strength. Antioxidant ability.	MIC: 50 and 2500 μg/mL for AgNPs and ZnONPs respectively. Inhibition zone: ~12 mm.	Non cytotoxic to HFs. Significant HFs migration and proliferation on the wound margin in vitro. Good hemocompatibility.	[64]
Cotton pads doped with chitosan, CG ZnONPs (CG@ZnONPs).	CG@ZnONPs.	Size: 30–80 nm.	Improved cotton fibers stability, especially thermal.	Growth reduction: 63%.	Faster and almost complete healing in vivo. Higher expression of mature collagen fibers depositions on the newly formed epidermis.	[65]
Chitosan-bentonite-gelatin films incorporated with ZnONPs.	ZnONPs.	ND.	Smooth and compact surface. Flexibility. High water absorption capacity.	Antibacterial effect: ~99%. Reduction logarithm: 2.69–3.28.	Non cytotoxic to L929 cells. Complete wound healing and re-epithelization (with lower inflammation and more compressed collagen) in vivo.	[66]
Gelatin-PCL NFs containing Ce_2O_3 NPs.	Ce_2O_3NPs.	Size: ~20 nm. Zeta potential: +18 mV.	NPs release from NFs: 25–35% (day 1) to 80–90% (day 9).	MICs: 6.25 μg/mL (ATCC) and 12 μg/mL (clinical isolate). MBCs: 50 μg/mL (ATCC) and 100 μg/mL (clinical isolate). Decreased the expression of the genes related to antibiotic resistance.	Non cytotoxic to HU2 cell line.	[67]
Hybrid nanocomposite containing $Mg(OH)_2$NPs embedded in a carboxymethyl cellulose hydrogel plus SF.	$Mg(OH)_2$NPs.	ND.	Improved mechanical properties, hydrophilicity, and water uptake capacity. Tensile strength, and elongation at break.	High-level potential in constraining the biofilm formation.	Non cytotoxic to HU2 cells. Good hemocompatibility. Faster wound healing in vivo.	[68]

Chitosan hydrogel containing Cur-Cu NPs-loaded niosomes.	Cur-CuNPs-Nio.	Size: 197.5 ± 6.42 nm. EE for Cur: 92.25 ± 1.22%.	Release: diffusion controlled release (Cur, ~40% in 72h) and Higuchi model (metal NPs, ~50% in 72h).	Zone of inhibition: 33 ± 1.1 mm. MIC: 3.125 µg/mL. MBC: 6.25 µg/mL. Significant reduction of biofilm formation.	Non cytotoxic for HFF cell line.	[69]
Nanocomposite containing MFA loaded CuNPs.	MFA-CuNPs.	Size: 312 nm. Zeta potential: −0.7 mV.	Cosmetically appealing appearance and smooth and homogeneous texture. Good spreadability, stickiness, bloom strength, and extrudability.	Inhibition zone: 17–20 mm.	Non cytotoxic for Vero cell line.	[70]
Pluronic F-127 hydrogel loaded with AgNPs coated with mercaptosuccinic acid.	AgNPs.	Core diameter: 2.98 ± 0.85 nm. Highly stable nature.	Shear-thinning behavior, porous structure and enhanced mechanical properties. Release profile: fast release in the first 10 h (~50%) + slow continuous release (<10%) for up to 24 h. Homogeneous distribution of AgNPs.	Inhibition zone: 18 mm. Bacterial death >97%. Biofilm disruption and elimination were a concentration-dependent phenomenon. High level of intracellular ROS by 35%.	Non cytotoxic to HFFs and HaCaTs. No significant changes in cell morphology and the associated actin cytoskeletal structure.	[21]
BC hydrogels loaded with AgNPs.	AgNPs.	Shape: spherical with smooth edges. Size: 42.71 ± 17.97 nm. Zeta potential: −21 ± 0.702 mV.	Fine fiber network structure with voids. High moisture content (98.86%). Antioxidant ability. Transparent.	Inhibition zone: 16 mm.	Non cytotoxic to Panc 1, U251, and MSTO cell lines Hemolytic material (6.85 ± 1.12%).	[23]
Chitosan, SA and SF dressing loaded with a compound of Exo and AgNPs.	AgNPs.	Size: 10–15 nm.	Moisture retention and electrolyte balance maintenance. Asymmetric dressing with a hydrophobic area and a hydrophilic area. Good porosity (60–70%). Slow release of AgNPs-Exo at the wound site (~70% in 72h). Secondary infection prevention thanks to the hydrophobic surface.	Halo size growth inhibition (not quantified). After treatment, the bacterial membrane was broken and the surface had pores.	Non cytotoxic to L929 cells, HFs and HUMSCs. Did not cause sensitization or allergic reactions. Promoted in vivo wound healing, cell proliferation and vascular regeneration. Epidermis completely repaired and keratinized at day 12.	[27]

(*Continued*)

https://doi.org/10.2147/IJN.S469724

Table 3 (Continued).

Wound Dressing	Antimicrobial Agent	NPs Properties	Most Significative Wound Dressing Properties	Antimicrobial Efficacy	Biocompatibility	Ref.
Fumaric acid incorporated agar-Ag hydrogel.	AgNPs.	Size: 11.55 ± 1.56 nm. Shape: spherical.	Preserved shape and size of AgNPs inside the gel. Antioxidant capacity. Spreadable and easy to apply. Moderate to slow degradation with slow Ag-release.	Inhibition zone: 20 mm. MIC:15.5 mg/mL.	Non cytotoxic to 3T3-L1 cells. No external toxicity appeared on skin. Non apoptotic to NHDF cells. Promoted in vivo wound healing by better tissue proliferation, more granulation tissue formation, neovascularization and mature collagen bundles.	[29]
Carbohydrate polymer-based silver nanocomposite hydrogels/Guar gum-grafted-polyacrylamide glycolic acid polymer, $AgNO_3$ and sodium borohydride.	AgNPs.	Well-monodispersed. Uniform morphology. Shape: spherical. Size: 5.4 ± 0.25 nm.	Self-healing ability, injectability, stretchability, flowability, high swelling, adhesion, good porosity, upright mechanical behavior, and biodegradability. Brown gel with soft and spongy textures. Hydrophobic surface.	Inhibition zone: ~18 mm.	Non cytotoxic to CCD-986sk cells.	[39]
Thermosensitive and injectable hydrogels based on HA, Pluronic, corn silk extract and AgNPs.	AgNPs.	Well-dispersed. Shape: spherical. Size: 13 ± 1 nm.	Good mechanical properties with gelation temperature close to body temperature. Low viscosity at high shear rate and upon the storage.	Excellent growth inhibitory effect.	Non cytotoxic to L929 cells. In vitro faster wound closure and repair.	[36]
Hybrid hydrogels based on maleic acid-modified dextran and thiolated chitosan loaded with AgNPs.	AgNPs.	ND.	Slow and sustained Ag^+ release (3.5–1 µg/L during 72 h). High porous structure. Unique antifouling property and excellent water absorption.	~100% bacterial death after 60 min. Bacterial surface shriveled and died.	Non cytotoxic to NIH 3T3 cells. Promoted in vivo wound healing improving fibroblast migration, granulation tissue formation and angiogenesis. In vivo modulate immune responses.	[28]
Chitosan- PEG hydrogel loaded with AgNPs.	AgNPs. + Chitosan.	Diameter in hydrogel: 99.1 ± 2.3 nm. Uniform distribution all along the hydrogel.	High porosity (72.2%), high degree of swelling and good WVTR. Slow and sustained release of AgNPs for 7 days. Slow biodegradation of hydrogels.	Inhibition zone: 21.8 ± 1.5 mm.	Complete tissue remodeling, re-epithelialization, collagen deposition, blood vessels and fewer inflammatory cells in vivo.	[31]

PVA and sodium alginate patch containing Cur tagged TiO_2 NPs (TiO_2 -Cur NPs).	TiO_2-Cur NPs.	Size: ~20 nm. Zeta potential: −57.4 mV.	Controlled release of Cur followed by the burst of TiO_2. Good swelling rate. Increased tensile strength.	Inhibition zone: 17 mm.	Non cytotoxic to NIH3T3 cells. Good hemocompatibility. Remodeling of the epidermis, progressive wound contraction and healing in vivo.	[71]
Hydrogel (Poloxamer 407) loaded with AuNPs.	AuNPs, Au nanorods (AuNRs).	Average length: ~49.2 ± 1.8 nm. Average width: ~12.9 ± 0.7 nm. Zeta potential: −32.6 and −1.2 mV for PAH-AuNRs and PEG-AuNRs, respectively. Release: slow and constant (first 24 h, ~55%) and complete after 48 h. Good colloidal stability	ND.	Reduction of bacterial viable count: ~99%.	Significant reduction of the wound after 7 days in vivo. No scars and rapid growth of adnexal structures after 21 days. Good re-epithelialization, well-developed granulation tissue with more stroma and less inflammatory cells. Abundant collagen deposition.	[72]

Abbreviations: 3T3-L1, mouse embryo fibroblasts; AD-L, guanidinium derivative with pyridine moieties; AgNC, silver nanoclusters; $AgNO_3$, silver nitrate; AgNPs, silver nanoparticles; AuNRs, gold nanorods; AuNPs, gold nanoparticles; BC, bacterial cellulose; C_3N_4, carbon nitride; CCD-986sk, human fibroblast skin cell line; Ce_2O_3NPs; cerium oxide nanoparticles; CG, glycogen; CS, *Camellia sinensis*; CuNPs, copper nanoparticles; Cur, curcumin; EE, entrapment efficacy; Exo, exosomes; Fe_2O_3 NPs; iron oxide NPs; GA, gum arabic; HaCaTs, human immortalized keratinocyte cell line; HA, hyaluronic acid; HACC, hyaluronic acid mixed with quaternized chitosan; HFs, human fibroblasts; HFF, human fibroblast foreskin cell line; hKTs, human keratinocytes; HPMC, hydroxypropyl methylcellulose; HU2; human fibroblast cell line; HUMSCs, human umbilical cord mesenchymal stem cells; HUVECs, human umbilical vein endothelial cells; LAB, *Lactobacillus acidophilus*; L929 cells, mouse fibroblast cell line; MBC, minimum bactericidal concentration; MBIC, minimum biofilm inhibitory concentration; MEF, mouse embryonic fibroblasts; MFA, mafenide acetate; $Mg(OH)_2$NPs, magnesium hydroxide nanoparticles; MIC, minimum inhibitory concentration; MSTO, human mesothelioma cell line; ND, not determined; NF, nanofibers; NHDF, normal adult human primary dermal fibroblasts; NIH3T3: fibroblasts from a mouse NIH/Swiss embryo; NPs, nanoparticles; PAH, poly allyl amine hydrochloride; Panc 1; human pancreatic ductal adenocarcinoma cell line; PCL, poly(ε-caprolactone); PEG, poly(ethylene glycol); PVA, polyvinyl alcohol; RAW 264.7, murine macrophages; Ref, reference; ROS, reactive oxygen species; SA, stearic acid; Se, sericin; SF, silk fibroin; SNPNPs, silver nitroprusside nanoparticles; THP-1, human macrophage cell line; TiO_2, titanium oxide; U251, human glioblastoma cell line; Vero-E6, epithelial cells; WVTR, water vapor transmission rate; ZnONPs, zinc oxide nanoparticles.

https://doi.org/10.2147/IJN.S469724

Silver NPs

A total of 28 papers on the evaluation of AgNP-loaded wound dressings were identified. They were found not to be cytotoxic in vitro against various cell types, including mouse fibroblasts (L929 cells,[18,20,22,26,27,34,38,61] 3T3-L1,[29] NIH 3T3[28,54]), HFs (NHDF,[29] CCD-986sk,[39] HFs,[27,56] HFFs,[21] MSTO), keratinocytes (HaCaTs[19,21,38]), endothelial cells (HUVECs[19]), epithelial cells (Vero-E6,[33,57] Panc 1[23]), macrophages (RAW 264. 7[32,38]), and mesenchymal cells (HUMSCs[27]). The commercial Acticoat™ dressing exhibited toxicity to hKT, which disqualifies it as a viable candidate.[58] Six of the papers evaluated hemocompatibility.[18–20,22,34,55] Gupta et al stated that their dressing was hemolytic and therefore does not meet one of the ideal characteristics of a good dressing.[23] Regarding in vivo results, two studies evaluated the absence of damage to vital organs,[24,34] while 13 studies have evaluated histological parameters such as re-epithelialization, collagen deposition, angiogenesis, and reduced presence of inflammatory cells.[19,20,22–24,26,27,29,31,34,54,62] Finally, the antioxidant capacity has been evaluated in five studies with positive results.[18,23,29,32,38]

In terms of the most significant ideal properties evaluated for wound dressings, 18 papers assessed moisture balance/swelling capacity,[19–23,26–28,31,32,34,38,39,53,54,56,57] and 11 papers reported high porosity.[19,21,22,26–28,31,32,39,54] 16 studies evaluated the biomechanical properties,[18–22,26,29,32–34,36,38,39,54,62] while eight papers analyzed the Ag ion release pattern.[21,27–29,31,32,34,62] Additionally, five papers evaluated biodegradability,[20,22,26,39,62] and seven studies provided stability data.[19,22,24,32,38,57,62] Three papers did not provide any data on these parameters.[55,58,61] Therefore, the most evaluated properties were moisture balance/swelling capacity and biomechanical properties. Regarding porosity, Singh et al did not show high values, which are desirable for a good dressing (15%),[38] while those showing higher porosity were 72.2%[31] and 72.6%.[26] The capacity to be 3D bioprinted was also demonstrated.[54,56]

Although all studies demonstrated antimicrobial activity against the microorganism of interest, they employed different techniques. In particular, 14 papers used the agar disk diffusion assay.[18,20,21,23,24,26,27,29,31,39,54,56,57,62] Overall, the antimicrobial efficacy of the NPs was enhanced when incorporated into the hydrogel. This resulted in bacterial inhibition zones ranging from 6 mm[56] to 27 mm.[26] Seven papers evaluated the MIC[18,29,32,33,53,55,61] and three papers assessed the minimum bactericidal concentration (MBC), defined as the lowest concentration of the hydrogel that does not show colony growth in the culture medium.[32,33,53] Although the importance of biofilm elimination has been recognized, only four papers[21,22,32,33] reported the ability of the hydrogel to eradicate biofilm formation. Some studies evaluated bacterial death using live/dead assays, achieving over 80% death.[19,21,28] Other methods included optical density measurements by turbidity tests,[22,34,36] observation of pores in the bacterial membrane by microscopy,[27,28,34] plate count assays[38] and time-kill assays.[55,56] It should be noted that bacterial growth was observed in the commercial Acticoat™ dressing,[58] indicating that its ability to eliminate bacteria was no better than the other experimental dressings evaluated in this review.

Others Inorganic NPs

A total of 12 studies have been conducted evaluating wound dressings loaded with other metallic NPs. These inorganic NPs include iron (Fe),[59,60] zinc (Zn),[63–66] copper (Cu)[69,70] cerium (Ce)[67] and titanium (Ti)[71] oxides, magnesium hydroxide ($Mg[OH]_2$)[68] and gold (Au) NPs.[72] The analyzed wound dressings, like those loaded with AgNPs, were biocompatible in vitro not only with mouse fibroblasts,[59,63,66,71] HFs[60,64,69] and epithelial cells[70] but also with urothelial cells.[67,68] Furthermore, $Mg(OH)_2$,[68] ZnO,[65,66] TiO_2[71] and Au[72] NPs-loaded wound dressings have shown rapid and complete re-epithelialization in vivo, with collagen deposition[65,66,72] and fewer inflammatory cells.[66,72]

Importantly, these wound dressings exhibited key properties. Iron oxide (IO) NPs-loaded dressings showed smooth surfaces[59] and when iron was incorporated in the form of MIL-53(Fe) NPs, they exhibited thermal stability, water retention and absorption ability and good mechanical strength.[60] These properties were also present in dressings incorporating ZnO,[64,66] $Mg(OH)_2$[68] and TiO_2[71] NPs. ZnONPs-loaded dressings also showed flexibility and antioxidant ability.[64] However, only CuONPs-loaded dressings showed good spreadability and extrudability. For dressings incorporating AuNPs, wound dressing properties were not evaluated.[72] Therefore, the most evaluated properties in this type of dressing were water retention and absorption ability and mechanical strength. Interestingly, only one study reported porosity in the developed dressing.[60]

The microbial activity of the remaining inorganic NPs was evaluated using various techniques; six papers assessed the agar disk diffusion assay,[59,60,63,69–71] which resulted in bacterial inhibition zones ranging from 17 mm[59] to 33 mm.[69] Additionally, six papers evaluated the MIC,[59,60,63,64,67,69] while five papers evaluated MBC.[59,60,63,67,69] Three papers analyzed the reduction of bacterial growth using optical density measurements by turbidity tests[65,66] or the viable bacterial count method,[72] In addition, four papers investigated the elimination of biofilm.[59,63,68,69] Of note is the study by Zamani et al, which evaluated the expression levels of genes involved in antibiotic resistance.[67]

Discussion

P. aeruginosa is a common hospital-acquired pathogen that causes life-threatening infections in critically ill patients. It is resistant to many drugs, making it challenging to treat. *P. aeruginosa* infections are common in healthcare settings and can cause significant morbidity and mortality.[1–3] Traditional treatments of infected wounds involve the topical application of antibiotics, but this can lead to systemic toxicity and the development of resistance.[12,13] Advanced wound dressings containing antibiotic NPs have shown promise in overcoming these challenges. To be considered an "ideal" wound dressing, they should fulfil several criteria. These criteria include hemostatic capacity, absorption, adhesion, moisture retention, porosity, mechanical properties, pH, biodegradability, transparency, biocompatibility, and antimicrobial properties.[18,22–24,28,31,33,38,39] These properties are crucial in promoting wound repair, improving wound appearance, and reducing healing time. Both natural (such as chitosan, cellulose, collagen, HA, gelatin, alginate, dextran, pullulan, agarose and SF) and synthetic polymers (including polyvinyl alcohol, PCL, PEG, PLGA and PDA) provide these features to the dressings. This systematic review focuses on the latest advances in the development of NPs-based wound dressings for the treatment of *P. aeruginosa* infected skin wounds.

In this sense, different types of wound dressings loaded with NPs were identified and analyzed, including organic (carbon-based and polymeric NPs) and inorganic (metallic, magnetic, metal oxides, metal hydroxide NPs and MOF). All of them exhibited antibacterial activity against *P. aeruginosa*. Figure 3 shows the percentage of publications by date for different wound dressings loaded with NPs. In particular, the 61.2% of the studies evaluated metallic NPs-loaded wound dressings. The next group with a higher percentage of publications is that evaluating polymeric NPs-loaded wound dressings (14.3%) followed by metal oxides NPs-loaded wound dressings (12.2%) and carbon-based NPs-loaded wound dressings (6.1%). Magnetic, metal hydroxides NPs and MOF represent 2% of the publications analyzed. It is noteworthy that most of the recent publications belong to the group of metallic NPs-loaded wound dressings.

Antibacterial activity was determined through different methods and evaluations including MIC and MBC determinations, bacterial kill assays, agar diffusion methods, live/dead assays and biofilm reduction or inhibition evaluations. It

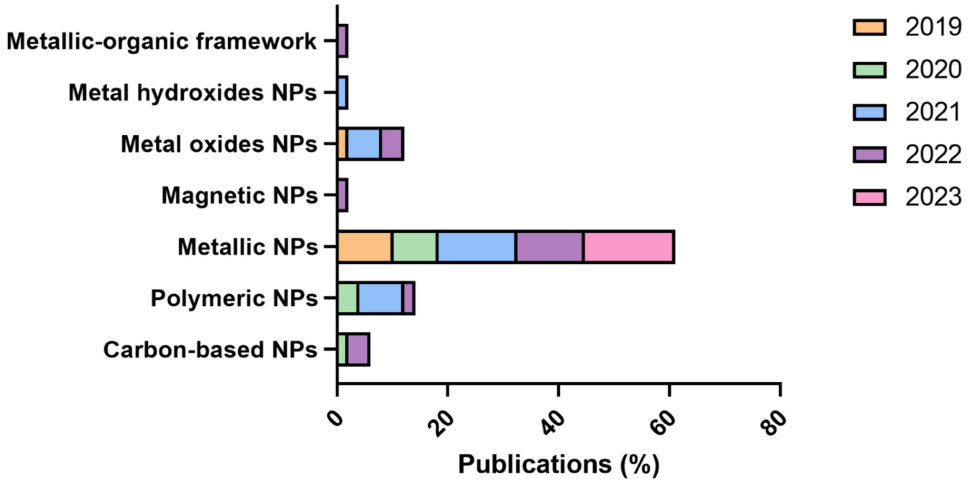

Figure 3 Percentage of publications by date of NPs-loaded wound dressings against *P. aeruginosa*. The studies reviewed focused on wound dressings loaded with different types of NPs: 61.2% with metallic NPs, 14.3% with polymeric NPs, 12.2% with metal oxides NPs, and 6.1% with carbon-based NPs. Magnetic NPs, metal hydroxides, and MOF accounted for 2% of the publications.

should be highlighted that biofilms can resist antibiotics and immune system clearance, leading to delayed wound healing and chronic inflammation.[9,73] As described above, their formation is mediated by the bacterial virulence factors and regulated by quorum-sensing mechanisms[74] and their dispersal can exacerbate disease, leading to acute life-threatening conditions.[75] It is therefore crucial to evaluate how NPs- loaded wound dressings affect *P. aeruginosa*'s biofilm. Despite this, only nine of the 49 studies identified in this systematic search, carried out this evaluation.[21,22,32,33,48,49,59,63,69]

Focusing on the reported wound dressings loaded with NPs, three studies regarding carbon-based NPs-loaded dressings were found in this search. These include GQDs and C-dots. GQDs are carbon-based zero-dimensional fluorescent nanomaterials with a graphene lattice inside.[76] They are very small, usually less than 20 nm and can easily penetrate through biological membranes and exhibit antimicrobial activity through the oxidative stress caused by the generation of ROS following their photoexcitation.[43,76] Besides being antimicrobial, these carbon-based dressings have shown not only biocompatibility in vitro and in vivo but also promotion of angiogenesis in vivo. This may be attributed to their ability to interact with ROS in wound tissue, leading to a reduction in ROS levels and activation of cell signaling molecules such as hypoxia-inducible factor 1α (HIF-1α) and the p38MAPK/Akt pathway, which enhances the production of angiogenic factors.[77] C-dots are generally defined as carbon nanomaterials composed of quasi-spherical carbon NPs.[78] As with GQDs, the antimicrobial mechanism of photoinduced C-dots includes the production of ROS, the disruption and penetration of the bacterial membrane and the induction of oxidative stress with damage to bacterial DNA.[78] They are also able to suppress bacterial proliferation by removing Fe^{3+} ions from the environment.[45] It is important to note that the incorporation of these NPs into wound dressings may be more costly than traditional methods that do not involve NPs.

Inorganic NPs incorporated into wound dressings include magnetic NPs (iron oxide NPs, IONPs), metallic-organic framework (MOF), metal oxides NPs (Zn, Cu, Ce and Ti oxides), metal hydroxides NPs ($Mg[OH]_2$) and metallic (Au, Cu and Ag) NPs. Specifically, this review has identified a total of 39 studies in which these types of dressings were developed and evaluated.

Ag is a well-known antimicrobial agent against fungi, yeasts, and bacteria, including antibiotic-resistant strains.[23] Researchers in various fields have widely used AgNPs for the treatment of infections due to their broad-spectrum antibacterial capacity.[22] The traditional synthesis of these NPs involves toxic organic solvents and reducing agents. However, there is a growing interest in "green chemistry synthesis" using natural substances, such as plant extracts and microorganisms, which are fast, economical, safe, and environmentally friendly.[38] For example, Cur extracted from turmeric has antimicrobial, antioxidant, and anti-inflammatory effects and can be used to reduce and protect Ag during NPs synthesis, enabling combined therapy with a synergistic effect.[19,20,23] AgNPs exert their antimicrobial effect by increasing the permeability of the bacterial cell membrane, interfering with DNA replication by binding to phosphorus-containing compounds, denaturing proteins, and releasing Ag ions inside the bacteria, which enhances their bactericidal effect.[23] They bind directly to the thiol groups of different biomolecules, including peptides, DNA, cofactors, and oxidized glutathione (GSH) to form glutathione disulphide (GSSG). This leads to increased levels of ROS, which in turn causes additional damage to bacteria.[26]

Importantly, AgNPs not only have antibacterial properties but also possess anti-inflammatory capacity. They prevent the expression of pro-inflammatory factors such as tumor necrosis factor alpha (TNF-α), interleukins 6 and 1ß, which accelerates wound healing by promoting the proliferation and migration of keratinocytes to the wound site.[24,26,39] Additionally, they induce the transformation of fibroblasts into myofibroblasts, leading to wound contraction. It is important to note that Gram-negative bacteria are more susceptible to the effects of Ag than Gram-positive bacteria. This may be because Gram-positive bacteria have a plasma membrane coated with a peptidoglycan layer, which may limit the penetration of AgNPs.[18,37]

However, despite being highly antibacterial and their anti-inflammatory ability, they are not stable in water and tend to agglomerate. Incorporating them into a hydrogel could reduce this issue.[39] Moreover, their use is still limited because they can pass through biological mucosal surfaces and penetrate animal organs. Therefore, it is recommended to use them in the lowest possible concentration to ensure sustained release.[27] These characteristics would also be improved by incorporating them into a biomaterial.

Other inorganic NPs include MOFs, IONPs, ZnONPs, Ce_2O_3NPs and TiO_2NPs, $Mg(OH)_2$NPs, CuNPs and AuNPs. These metal-based NPs are valuable for biofilm inhibition and treatment of microbial diseases due to their ultra-small

size and high surface area.[59,79] IONPs are highly promising for antimicrobial therapy because of their strong magnetic and semiconductor properties.[59] Magnetic fields cause bacterial death and biofilm eradication through vibration damage, local hyperthermia, and ROS production.[80] A MOF-based hydrogel was reported in this systematic review. Specifically, a carboxylic acid iron MOF, called MIL-53(Fe), which is made from iron ions and terephthalic acid. These frameworks are a distinct type of hybrid materials formed by combining inorganic and organic components[60] and are well-suited for biomedical applications due to their specific characteristics, such as high porosity, high surface area, customizable chemical surface, good compatibility with the physico-chemical interaction of drugs, and interconnected channels suitable for use in drug loading and release systems.[60] In addition to causing physical damage to bacterial cells through direct contact, they can also store and slowly release metal ions, leading to the generation of oxidative stress and/or photothermal effects.[81,82] ZnONPs have been reported as antimicrobial and anti-inflammatory agents and also, to play a role in fibroblast proliferation, angiogenesis, and increased re-epithelialization.[63,64] Their antibacterial mechanism is mediated by direct contact with bacterial membranes, resulting in destruction of cell integrity, release of antimicrobial ions, mainly Zn^{2+} ions, and ROS generation.[83] Ce_2O_3 is a natural scavenger of free radicals such as ROS and reactive nitrogen species (RNS). Ce_2O_3NPs are likely to exert their antibacterial mechanism by inducing oxidative stress and interfering with the nutrient transport functions.[84] Furthermore, unlike TiO_2NPs which required photoactivation, Ce_2O_3NPs exhibit antibacterial effect without external activation.[85] The photoactivation of TiO_2NPs is possible due to its good photocatalytic activity in the anatase phase. As a result, these NPs produce ROS that destroy the bacterial outer membrane and ultimately destroy the bacterial cell.[71,86]

$Mg(OH)_2$NPs have been reported as an approved drugs and food additives due to their excellent biocompatibility, low toxicity, thermal stability and low cost of production.[68,87] They are effective agents against several bacteria, including *P. aeruginosa*, exerting their antibacterial activity through two potential mechanisms. The first mechanism involves the direct infiltration of the NPs into the cell membrane, causing membrane damage and resulting in cell death. The second mechanism involves the absorption of water moisture on the surface of the NPs, creating a thin layer of high pH water that can harm bacterial membranes.[88] Nevertheless, this antibacterial mechanism is still unclear.[87] In fact, only one study has evaluated the incorporation of these NPs into a wound dressing and analyzed its properties, biocompatibility and antibacterial capacity.[68] Cu and AuNPs were also reported in this systematic review as inorganic NPs based wound dressings. CuNPs are known to have the highest antimicrobial property among the known synthesized metal NPs, with high level of biocompatibility.[70] The antibacterial mechanism is based on the interaction of Cu with amine and carboxyl groups on the surface of microbial cells, the inhibition of amino acid synthesis, and the inactivation of microbial proteins through thiol interaction.[69] Like Cu, the main antimicrobial mechanism of AuNPs is based on the direct adhesion of AuNPs to the bacterial surface, driven by electrostatic forces.[89] These NPs are colloidal or clustered particles composed of a Au core with high synthetic versatility and non-toxic nature.[72,89]

Taken together, all the studies evaluating wound dressing containing inorganic NPs showed biocompatibility with several cell lines and antibacterial activity. Nevertheless, only 18 out of 39 (46.1%) studies performed in vivo evaluations. Therefore, more research is needed to confirm the beneficial role of these dressings in vivo.

In addition to the proposed mechanisms, emerging therapies are gaining attention to enhance the antibacterial capacity of metallic NPs due to their high target selectivity, minimal invasiveness and reduction in bacterial drug resistance.[90] These include photothermal therapy (PTT), photodynamic therapy (PDT) and chemodynamic therapy (CDT).

PTT uses photoinduced heat to destroy bacterial pathogens and is generally developed by combining a near infrared (NIR) laser with highly effective NIR light-absorbing nanomaterials.[91] Several studies have employed this strategy against Gram-negative bacterial infections including *P. aeruginosa* infections. For instance, He et al reported efficient bactericidal and anti-biofilm effects by photothermal enhancement and ROS generation of high-entropy transition metal carbides or nitrides (HE MXenes) monolayers that eradicated methicillin-resistant *Staphylococcus aureus* infected tissue inflammation and stimulated angiogenesis in vivo.[92] With regard to *P. aeruginosa* infections, Ye et al developed CuO- and AgO-doped ZnO nanocomposites that exhibited excellent photothermal stability and intrinsic antibacterial activity.[93] Another strategy in this field was carried out by Lv et al who developed a nanorod based on molybdenum disulphide nanosheets coated with AuNRs to target lipopolysaccharide present on the surface of bacteria, demonstrating a strong photothermal effect as well as a more significant antibacterial effect than non-targeted PTT.[94]

PDT employs a photosensitizer that absorbs light energy and transfers it to oxygen to produce ROS, resulting in bacterial cell death.[90] Cur has been used as a photosensitizer in combination with silica,[95,96] AgNPs[97,98] and GQT[99] to combat planktonic, biofilm and clinical isolates of *P. aeruginosa* showing promising results for the application of this therapy in vivo. AgNPs have also been photosensitized with methylene blue.[100] GQT,[99] AuNPs[101] and ZnONPs[102] have also been reported to play the role of photosensitizer achieving broad antibacterial efficacy and strong biofilm inhibition after light irradiation. All these studies used visible light to activate the photosensitizer, which may result in poor tissue penetration.

Garin et al[103] proposed the combination of PDT with PTT by using copper sulphide NPs together with indocyanine green activated in the NIR region of the electromagnetic spectrum for the elimination of *P. aeruginosa* to reach superior tissue penetration. This kind of therapy combination was also reported by Mo et al[104] who developed a C_7S_4 nanosheet with excellent antibacterial activity through synergistic PDT and PTT against drug-resistant *P. aeruginosa* under NIR light irradiation, which inhibited skin infection in mice.

CDT, also known as peroxidase-mediated chemokinetic therapy refers to the ability of metallic NPs to produce hydroxyl radicals that damage bacterial cells. These NPs with peroxidase activity are also known as nanozymes. However, the antibacterial effects of these nanozymes are limited due to the insufficient production of hydroxyl radicals and the short range of action.[104] PTT can improve the catalytic activity of nanozymes by stimulating them with NIR light. For example, He et al combined the photothermal potential of V_2C MXene nanosheets with the chemodynamic activity of platinum (Pt) NPs to create a Pt@V_2C platform with enhanced antibacterial properties.[105] Furthermore, Liu et al irradiated with a NIR laser $CuFeS_2$ NPs to stimulate their peroxidase activity achieving more than 99% inactivation efficiency of *P. aeruginosa* through the combination of PTT, PDT and also by consuming intracellular glutathione in bacteria, resulting in more ROS production.[106]

In addition to the dual therapies, a combination of PTT, PDT and CDT was also reported against *P. aeruginosa*. Dai et al developed a NIR-activated multimodal agent by loading fluorescein isothiocyanate, ultrasmall copper sulfide NPs (Cu_2−xSNPs), and ε-polylysine onto mesoporous silica NPs.[107] This agent could detect the bacteria and biofilms by fluorescence imaging, ablate bacteria and biofilms and treat bacterial infections in vivo.

However, despite the advances that these therapies offer in terms of superior antibacterial activity, high tissue penetration and biocompatibility, only one study identified in this systematic review applied PDT by using visible light irradiation of C_3N_4 to improve the antibacterial activity of AgNPs- loaded wound dressing.[34] Therefore, the combination of these therapies in the field of NPs-loaded wound dressings against *P. aeruginosa* infection needs to be further investigated.

Finally, this systematic review reported 7 strategies of polymeric NPs-loaded wound dressings including PDA NPs,[46,50] chitosan NPs,[47–49] sodium alginate NPs[51] and PLGA NPs.[52] Polymeric NPs range in size from 1 to 1000 nm and can be loaded with active compounds or drugs that are entrapped within the polymeric core or surface-adsorbed.[108] This review reported that CIP,[50,52] cefepime[47] and polymyxin B[51] are the main encapsulated drugs used in wound dressings against *P. aeruginosa* skin infections. Surprisingly, non-encapsulated polymeric NPs have also shown antibacterial activity.[46,48,49] These polymeric NPs are biocompatible, as supported by the results, and biodegradable, properties that are crucial for wound healing strategies. For PLGA NPs, the degradation rate, mechanical strength and drug loading and release kinetics can be precisely adjusted by altering the ratio of lactic acid to glycolic acid.[109] Chitosan is a mucoadhesive cationic linear polysaccharide and is one of the most widely used natural polymeric-based NPs for drug delivery due to its low cost, biodegradability, and availability in a wide range of molecular weights. It also has inherent antimicrobial and antioxidant capacities.[48,49,110] Alginate is an anionic mucoadhesive polysaccharide with versatile physicochemical properties that allow chemical modification for site-specific targeting.[111] Finally, PDA NPs are produced by the oxidative self-polymerization of dopamine and are employed in the manufacture of wet adhesive hydrogels. They improve the mechanical and self-healing properties of the hydrogels by exploiting reversible non-covalent interactions such as π–π stacking and hydrogen bonding.[46,112]

Table 4 summarizes the benefits and drawbacks of the different strategies of NPs-loaded wound dressings against *P. aeruginosa* skin infection. Their antimicrobial mechanisms are represented in Figure 4.

Table 4 Benefits and Drawbacks of NPs-Loaded Wound Dressings Against *P. aeruginosa*

Wound Dressings	NPs	Benefits	Drawbacks
Carbon-based NPs-loaded wound dressings.	GQD.	NPs can easily penetrate through biological membranes thanks to their ultra-small size. Antimicrobial activity after photoexcitation. Photothermal performance. Biocompatible in vitro and in vivo. Angiogenic.	Need to be photoexcited to display the antimicrobial effect. Biofilm reduction to be evaluated. Expensive incorporation to wound dressing.
	C-dots.	Antimicrobial activity after photoexcitation and through Fe^{3+} sequestration from the environment. Capability of being 3D bioprinted. Biocompatible in vitro.	No biocompatibility was determined in vivo. Biofilm reduction to be evaluated. Expensive incorporation to the wound dressing.
Polymeric NPs-loaded wound dressings.	PDA.	Biocompatible in vitro and in vivo. Porosity, thermal and mechanical stability, and self-healing capacity. Water retention.	Only 1 study evaluated biocompatibility in vivo. Biofilm reduction to be evaluated.
	PLGA.	The degradation rate, mechanical strength and drug loading can be adjusted by altering the ratio lactic acid: glycolic acid. Biocompatible in vitro. Prevents invasiveness in vitro.	No biocompatibility was determined in vivo. Wound dressing properties to be evaluated. Biofilm reduction to be evaluated.
	Chitosan.	Thermal and mechanical stability. Water retention. Biocompatible in vitro and in vivo. Biofilm evaluation. Low cost.	1 study showed porosity below ideal values.
	Sodium alginate.	Versatile physicochemical properties. Biocompatible in vitro and in vivo. Adequate mechanical properties.	Biofilm reduction to be evaluated.

(*Continued*)

https://doi.org/10.2147/IJN.S469724

Table 4 (Continued).

Wound Dressings	NPs	Benefits	Drawbacks
Inorganic NPs-loaded wound dressings.	AgNPs.	Fast, economical, and environmentally friendly synthesis. Variety of antimicrobial mechanisms. Efficient against antimicrobial-resistant strains. Anti-inflammatory capacity. Biocompatible in vitro and in vivo.	Need to be incorporated in hydrogels to avoid agglomeration. Need to use in their lowest concentration to avoid extravasation to healthy tissues. Only 4 studies evaluated biofilm reduction.
	CuNPs.	Biocompatible in vitro. Cosmetical appearance. Good spreadability, stickiness, bloom strength, and extrudability. Antimicrobial capacity by the interaction with the bacterial membrane.	No biocompatibility was determined in vivo. Biofilm reduction to be evaluated.
	AuNPs.	Biocompatible in vivo. Good colloidal stability. High synthetic versatility. Antimicrobial capacity by the interaction with the bacterial membrane.	Biofilm reduction to be evaluated. Wound dressing properties to be evaluated.
	IONPs.	Magnetic and semiconductor properties. Biocompatible in vitro. Biofilm inhibition evaluation.	No biocompatibility was determined in vivo. Wound dressing properties to be evaluated.
	MOF.	Chemical versatility and large capacity for drug loading. Capacity for storing and slow release of metal ions Biocompatible in vitro. Porosity, thermal stability, mechanical strength and water retention.	No biocompatibility was determined in vivo. Biofilm reduction to be evaluated.
	ZnONPs.	Anti-inflammatory and angiogenic properties. Biocompatible in vitro and in vivo. Water absorption, flexibility and thermal stability of wound dressings.	Biofilm reduction to be evaluated.
	$Mg(OH)_2$NPs.	Low cost of production. Biocompatible in vitro and in vivo. Biofilm inhibition evaluation. Good mechanical properties and water absorption.	Antimicrobial mechanism to be clarified or defined.
	TiO_2NPs.	Antibacterial activity by inducing oxidative stress. Biocompatible in vitro and in vivo. Good swelling rate and increased tensile strength.	Need photo-activation to accomplish the antimicrobial effect. Biofilm reduction to be evaluated.
	Ce_2O_3NPs.	Biocompatible in vitro. Decreased the expression of the antibiotic resistance genes. Antibacterial activity by inducing oxidative stress. No need for photo-activation.	No biocompatibility was determined in vivo. Biofilm reduction to be evaluated. Wound dressing properties to be evaluated.

Abbreviations: AgNPs, silver nanoparticles; AuNPs, gold nanoparticles; C-dots, Carbon dots; Ce_2O_3NPs, cerium oxide nanoparticles; CuNPs, copper nanoparticles; GQD, graphene quantum dots; IONPs, iron oxide nanoparticles; $Mg(OH)_2$, magnesium hydroxide nanoparticles; NPs MOF, Metallic-organic framework; NPs, Nanoparticles; PDA, polydopamine; PLGA, poly(lactic-co-glycolic) acid; TiO_2NPs, titanium oxide nanoparticles; ZnONPs, Zinc oxide nanoparticles.

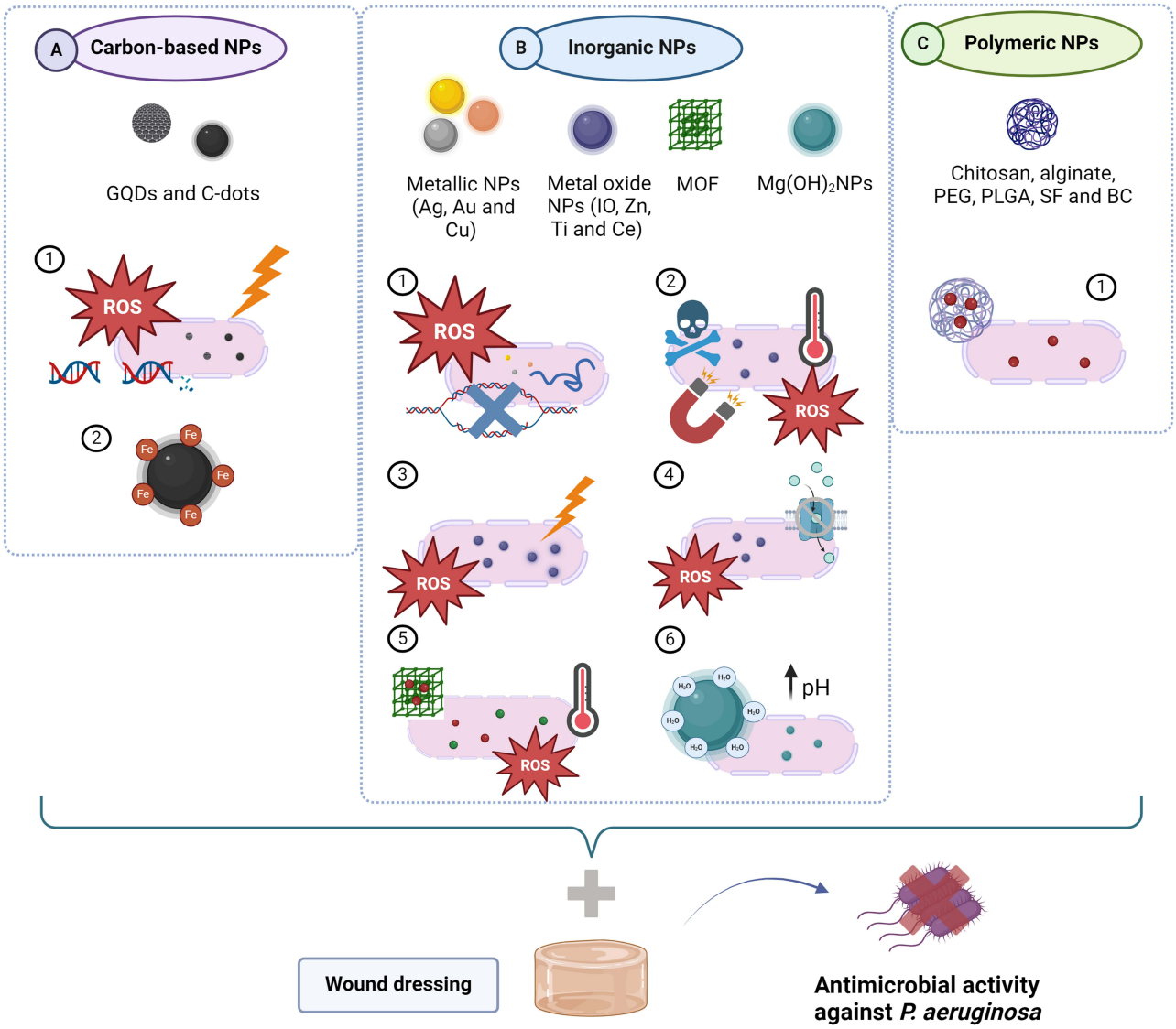

Figure 4 Main antimicrobial mechanisms of carbon-based, inorganic and polymeric NPs. (**A**). Carbon-based NPs: 1) ROS production after photoexcitation, bacterial membrane disruption and DNA damage (QGDs and C-dots) and 2) sequestration of Fe^{3+} from the environment (C-dots). (**B**) Inorganic NPs: 1) increment of membrane permeability after electrostatic adherence, interference with DNA replication, denaturation of proteins and ROS production (Metallic NPs); 2) ROS production, vibration damage, local hyperthermia (IONPs); 3) ROS production and nutrient transport inhibition (Ce_2O_3NPs); 4) destruction of cell integrity, liberation of metal ions and ROS generation without photoexcitation (ZnONPs) and after photoexcitation (TiO_2NPs); 5) bacterial damage after direct contact, drug and metal ions liberation, oxidative stress and photothermal effect (MOF) and 6) bacterial damage by direct infiltration of the NPs into the cell membrane and/or absorption of water moisture on NPs' surfaces, creating a thin layer of high pH water ($Mg[OH]_2$NPs). C. Polymeric NPs: 1) drugs and/or active compounds release. Created with biorender.com.

Conclusions

In the last 5 years and due to the advantages provided by the field of nanotechnology to reduce the problems of toxicity and resistance of conventional treatments, a variety of wound dressings loaded with NPs have been developed for the control of skin infections caused by *P. aeruginosa*, one of the most common nosocomial microorganisms in this type of infection. 79.6% (39/49) of these strategies use inorganic NPs as antibacterial agents, including metallic, metal oxide, metal hydroxide and magnetic NPs and MOFs. It is worth noting that among inorganic NPs, 71.8% (28/39) incorporate AgNPs into the generated dressings, possibly due to their properties and the diversity of antimicrobial mechanisms they possess, making them the most promising and advantageous NPs to incorporate into wound dressings. Disadvantages such as their toxicity and tendency to agglomerate require further research in this area. However, despite their advantages, only 14.2% of the studies developed dressings loaded with polymeric NPs and 6.1% with carbon-based

NPs. Importantly, despite the research carried out, there are still no clinical trials evaluating the efficacy of NPs-loaded wound dressings in patients. This may be because there are no universally accepted standards for assessing the specific risks associated with NPs.[77] Emerging therapies such as PPT, PDT or CDT and their combination have shown promising results against *P. aeruginosa* infection. However, only study to date has used PTT together with NPs-loaded wound dressings against this bacterium. Further research is therefore needed in this field to overcome these issues, ensure the safety of these treatments and ultimately translate the results of the investigations from the bench to the bedside.

Abbreviations

3T3-L1, mouse embryo fibroblasts; AD-L, guanidinium derivative with pyridine moieties; AgNCs, silver nanoclusters; $AgNO_3$, silver nitrate; AgNPs, silver nanoparticles; AuNRs, gold nanorods; AuNPs, gold nanoparticles; BC, bacterial cellulose; C_3N_4, carbon nitride; C60, carbon 60; CCD-986sk, human fibroblast skin cell line; C-dots, carbon dots; CDT, chemodynamic therapy; Ce_2O_3NPs; cerium oxide nanoparticles; CFU, colony-forming units; CG, glycogen; CIP, ciprofloxacin; CNCs, cellulose nanocrystals; CS, Camellia sinensis; CuNPs, copper nanoparticles; Cur, curcumin; EE, entrapment efficacy; Exo, exosomes; Fe_2O_3 NPs; iron oxide NPs; GA, gum Arabic; GQD, graphene quantum dots; GSSG, glutathione disulphide; GSH, oxidized glutathione; HA, hyaluronic acid; HaCaTs, human immortalized keratinocyte cell line; HACC, hyaluronic acid mixed with quaternized chitosan; HE MXenes, high-entropy transition metal carbides or nitrides; HFs, human fibroblasts; HFF, human fibroblast foreskin cell line; HGCs, human gingival cells; HIF-1α, hypoxia-inducible factor 1α; hKTs, human keratinocytes; hMSCs, human mesenchymal stem cells; HPMC, hydroxypropyl methylcellulose; HT1080 cells, epithelial cells derived from connective tissue from a patient with Fibrosarcoma; HU2; human fibroblast cell line; HUMSCs, human umbilical cord mesenchymal stem cells; HUVECs, human umbilical vein endothelial cells; L929 cells, mouse fibroblast cell line; IONPs, iron oxide nanoparticles; LAB, *Lactobacillus acidophilus*; MBC, minimum bactericidal concentration; MBIC, minimum biofilm inhibitory concentration; MC3T3-E1, mouse embryonic osteoblasts; MCRC-5 cells, human lung embryonic cells; MDR, multi-drug resistant; MEF, mouse embryonic fibroblasts; MFA, mafenide acetate; $Mg(OH)_2$NPs, magnesium hydroxide nanoparticles; MIC, minimum inhibitory concentration; MOF, metallic-organic framework; MSTO, human mesothelioma cell line; nChiD, nanochitosan dots; ND, not determined; NF, nanofibers; NHDF, normal adult human primary dermal fibroblasts; NIH3T3, fibroblasts from a mouse NIH/Swiss embryo; NIR, near infrared; NPs, nanoparticles; *P. aeruginosa, Pseudomonas aeruginosa*; PAH, poly allyl amine hydrochloride; Panc 1; human pancreatic ductal adenocarcinoma cell line; PCL, poly(ε-caprolactone); PDA, polydopamine; PDT, photodynamic therapy; PEG, poly (ethylene glycol); PL, poly-L-lysine; PLGA, poly(lactic-co-glycolic) acid; PRISMA, preferred reporting items for systematic reviews and meta-analyses; Pt, platinum; PTT, photothermal therapy; PVA, polyvinyl alcohol; RAW 264.7, murine macrophages; Ref, reference; ROS, reactive oxygen species; SA, stearic acid; SC, self-assembly confined; Se, sericin; SF, silk fibroin; SNPNPs, silver nitroprusside nanoparticles; WVTR, water vapor transmission rate; THP-1, human macrophage cell line; TiO_2, titanium oxide; TNF-α, tumor necrosis factor α; U251, human glioblastoma cell line; Vero-E6, epithelial cells; WHO, world health organization; WRI, wound refraction index; XL, xenon light; ZnONPs, zinc oxide nanoparticles.

Data Sharing Statement

All data generated or analyzed during this study are included in this article. Further enquiries can be directed to the corresponding author.

Author Contributions

All authors made a significant contribution to the work reported, whether that is in the conception, study design, execution, acquisition of data, analysis and interpretation, or in all these areas; took part in drafting, revising or critically reviewing the article; gave final approval of the version to be published; have agreed on the journal to which the article has been submitted; and agree to be accountable for all aspects of the work.

Funding

María I. Quiñones Vico's work is funded by a predoctoral fellowship (FPU19/05455, BOE 22 October 2019) from the Ministry of Science, Innovation and Universities of Spain. This research is part of her doctoral studies in the biomedicine

program at the University of Granada. We also acknowledge financial support from the Andalusian Regional Government (PIGE-0242-2019) and the Carlos III Health Institute (PI17/02083).

Disclosure

The authors declare that there are no conflicts of interest in this work.

References

1. Morand A, Morand JJ. Pseudomonas aeruginosa en dermatologie. *Ann Dermatol Venereol*. 2017;144(11):666–675. doi:10.1016/j.annder.2017.06.015
2. Sanya DRA, Onésime D, Vizzarro G, Jacquier N. Recent advances in therapeutic targets identification and development of treatment strategies towards Pseudomonas aeruginosa infections. *BMC Microbiol*. 2023;23(1):1–18. doi:10.1186/s12866-023-02832-x
3. Lynch JP, Zhanel GG, Clark NM. Emergence of antimicrobial resistance among pseudomonas aeruginosa: implications for therapy. *Semin Respir Crit Care Med*. 2017;38(3):326–345. doi:10.1055/s-0037-1602583
4. Karna SLR, Nguyen JQ, Evani SJ, et al. T3SS and alginate biosynthesis of Pseudomonas aeruginosa impair healing of infected rabbit wounds. *Microb Pathog*. 2020;147(104254):1–9. doi:10.1016/j.micpath.2020.104254
5. Botelho J, Grosso F, Peixe L. Antibiotic resistance in Pseudomonas aeruginosa – mechanisms, epidemiology and evolution. *Drug Resist Updat*. 2019;44:26–47.
6. Reynolds D, Kollef M. The epidemiology and pathogenesis and treatment of pseudomonas aeruginosa infections: an update. *Drugs*. 2021;81(18):2117–2131. doi:10.1007/s40265-021-01635-6
7. Spernovasilis N, Psichogiou M, Poulakou G. Skin manifestations of Pseudomonas aeruginosa infections. *Curr Opin Infect Dis*. 2021;34(2):72–79. doi:10.1097/QCO.0000000000000717
8. Serra R, Grande R, Butrico L, et al. Chronic wound infections: the role of pseudomonas aeruginosa and staphylococcus aureus. *Expert Rev Anti Infect Ther*. 2015;13(5):605–613. doi:10.1586/14787210.2015.1023291
9. Hoang TPN, Ghori MU, Conway BR. Topical antiseptic formulations for skin and soft tissue infections. *Pharmaceutics*. 2021;13(4):1–31. doi:10.3390/pharmaceutics13040558
10. Quiñones-Vico MI, Fernández-González A, Ubago-Rodríguez A, et al. Antibiotics against pseudomonas aeruginosa on human skin cell lines: determination of the highest non-cytotoxic concentrations with antibiofilm capacity for wound healing strategies. *Pharmaceutics*. 2024;16(1):1–18. doi:10.3390/pharmaceutics16010117
11. Torrens G, Hernández SB, Ayala JA, et al. Regulation of AmpC-Driven β -Lactam Resistance in Pseudomonas aeruginosa: different Pathways, Different Signaling. *mSystems*. 2019;4(6):1–14. doi:10.1128/mSystems.00524-19
12. Mofazzal Jahromi MA, Sahandi Zangabad P, Moosavi Basri SM, et al. Nanomedicine and advanced technologies for burns: preventing infection and facilitating wound healing. *Adv Drug Deliv Rev*. 2018;123:33–64. doi:10.1016/j.addr.2017.08.001
13. Souto EB, Ribeiro AF, Ferreira MI, et al. New nanotechnologies for the treatment and repair of skin burns infections. *Int J Mol Sci*. 2020;21(393):1–18. doi:10.3390/ijms21020393
14. Negut I, Grumezescu V, Grumezescu AM. Treatment strategies for infected wounds. *Molecules*. 2018;23(9):1–23. doi:10.3390/molecules23092392
15. Li X, Chen D, Xie S. Current progress and prospects of organic nanoparticles against bacterial biofilm. *Adv Colloid Interface Sci*. 2021;294(102475):1–19. doi:10.1016/j.cis.2021.102475
16. Zhou K, Li C, Chen D, et al. A review on nanosystems as an effective approach against infections of Staphylococcus aureus. *Int J Nanomed*. 2018;13:7333–7347. doi:10.2147/IJN.S169935
17. Yetisgin AA, Cetinel S, Zuvin M, Kosar A, Kutlu O. Therapeutic nanoparticles and their targeted delivery applications. *Molecules*. 2020;25(9):1–31.
18. Shi W, Kong Y, Su Y, et al. Tannic acid-inspired, self-healing, and dual stimuli responsive dynamic hydrogel with potent antibacterial and anti-oxidative properties. *J Mater Chem B*. 2021;9(35):7182–7195. doi:10.1039/D1TB00156F
19. Jiang M, Li S, Ming P, et al. Rational design of porous structure-based sodium alginate/chitosan sponges loaded with green synthesized hybrid antibacterial agents for infected wound healing. *Int J Biol Macromol*. 2023;237(123944):1–14. doi:10.1016/j.ijbiomac.2023.123944
20. Liu C, Zhu Y, Lun X, Sheng H, Yan A. Effects of wound dressing based on the combination of silver@curcumin nanoparticles and electrospun chitosan nanofibers on wound healing. *Bioengineered*. 2022;13(2):4328–4339. doi:10.1080/21655979.2022.2031415
21. Haidari H, Kopecki Z, Bright R, et al. Ultrasmall AgNP-impregnated biocompatible hydrogel with highly effective biofilm elimination properties. *ACS Appl Mater Interfaces*. 2020;12(37):41011–41025. doi:10.1021/acsami.0c09414
22. Huang Y, Bai L, Yang Y, Yin Z, Guo B. Biodegradable gelatin/silver nanoparticle composite cryogel with excellent antibacterial and antibiofilm activity and hemostasis for Pseudomonas aeruginosa-infected burn wound healing. *J Colloid Interface Sci*. 2022;608:2278–2289. doi:10.1016/j.jcis.2021.10.131
23. Gupta A, Briffa SM, Swingler S, et al. Synthesis of silver nanoparticles using curcumin-cyclodextrins loaded into bacterial cellulose-based hydrogels for wound dressing applications. *Biomacromolecules*. 2020;21(5):1802–1811. doi:10.1021/acs.biomac.9b01724
24. Rao BR, Kumar R, Haque S, et al. Ag2[Fe(CN)5NO]-Fabricated Hydrophobic Cotton as a Potential Wound Healing Dressing: an in Vivo Approach. *ACS Appl Mater Interfaces*. 2021;13(9):10689–10704. doi:10.1021/acsami.0c19904
25. Vivcharenko V, Przekora A. Modifications of wound dressings with bioactive agents to achieve improved pro-healing properties. *Appl Sci*. 2021;11(4114):1–16. doi:10.3390/app11094114
26. Chen X, Zhang H, Yang X, et al. Preparation and application of quaternized chitosan-and AgNPs-base synergistic antibacterial hydrogel for burn wound healing. *Molecules*. 2021;26(4037):1–16.
27. Qian Z, Bai Y, Zhou J, et al. A moisturizing chitosan-silk fibroin dressing with silver nanoparticles-adsorbed exosomes for repairing infected wounds. *J Mater Chem B*. 2020;8(32):7197–7212. doi:10.1039/D0TB01100B

28. Shi G, Chen W, Zhang Y, Dai X, Zhang X, Wu Z. An antifouling hydrogel containing silver nanoparticles for modulating the therapeutic immune response in chronic wound healing. *Langmuir*. 2019;35(5):1837–1845. doi:10.1021/acs.langmuir.8b01834
29. Basha SI, Ghosh S, Vinothkumar K, et al. Fumaric acid incorporated Ag/agar-agar hybrid hydrogel: a multifunctional avenue to tackle wound healing. *Mater Sci Eng C*. 2020;111(110743):1–13. doi:10.1016/j.msec.2020.110743
30. Liang Y, He J, Guo B. Functional Hydrogels as Wound Dressing to Enhance Wound Healing. *ACS Nano*. 2021;15(8):12687–12722. doi:10.1021/acsnano.1c04206
31. Masood N, Ahmed R, Tariq M, et al. Silver nanoparticle impregnated chitosan-PEG hydrogel enhances wound healing in diabetes induced rabbits. *Int J Pharm*. 2019;559:23–36. doi:10.1016/j.ijpharm.2019.01.019
32. Wunnoo S, Bilhman S, Waen-ngoen T, et al. Thermosensitive hydrogel loaded with biosynthesized silver nanoparticles using Eucalyptus camaldulensis leaf extract as an alternative treatment for microbial biofilms and persistent cells in tissue infections. *J Drug Deliv Sci Technol*. 2022;74(103588):1–16.
33. Dey A, Yadav M, Kumar D, et al. A combination therapy strategy for treating antibiotic resistant biofilm infection using a guanidinium derivative and nanoparticulate Ag(0) derived hybrid gel conjugate. *Chem Sci*. 2022;13:10103–10118. doi:10.1039/D2SC02980D
34. Liu C, Ling J, Yang LY, Ouyang Kun X, Wang N. Chitosan-based carbon nitride-polydopamine-silver composite dressing with antibacterial properties for wound healing. *Carbohydr Polym*. 2023;303(120436):1–13. doi:10.1016/j.carbpol.2022.120436
35. Luneva O, Olekhnovich R, Uspenskaya M. Bilayer Hydrogels for Wound Dressing and Tissue Engineering. *Polymers (Basel)*. 2022;14 (3135):1–36. doi:10.3390/polym14153135
36. Makvandi P, Ali GW, Della Sala F, Abdel-Fattah WI, Borzacchiello A. Biosynthesis and characterization of antibacterial thermosensitive hydrogels based on corn silk extract, hyaluronic acid and nanosilver for potential wound healing. *Carbohydr Polym*. 2019;223(115023):1–12. doi:10.1016/j.carbpol.2019.115023
37. Fereydouni N, Zangouei M, Darroudi M, Hosseinpour M, Gholoobi A. Antibacterial activity of chitosan-polyethylene oxide nanofibers containing silver nanoparticles against aerobic and anaerobic bacteria. *J Mol Struct*. 2023;1274(134304):1–11. doi:10.1016/j.molstruc.2022.134304
38. Singh S, Nwabor OF, Sukri DM, et al. Poly (vinyl alcohol) copolymerized with xanthan gum/hypromellose/sodium carboxymethyl cellulose dermal dressings functionalized with biogenic nanostructured materials for antibacterial and wound healing application. *Int J Biol Macromol*. 2022;216:235–250. doi:10.1016/j.ijbiomac.2022.06.172
39. Palem RR, Madhusudana Rao K, Kang TJ. Self-healable and dual-functional guar gum-grafted-polyacrylamidoglycolic acid-based hydrogels with nano-silver for wound dressings. *Carbohydr Polym*. 2019;223(115074):1–12. doi:10.1016/j.carbpol.2019.115074
40. Ahmad N. In vitro and in vivo characterization methods for evaluation of modern wound dressings. *Pharmaceutics*. 2023;15(42):1–47.
41. Laurano R, Boffito M, Ciardelli G, Chiono V. Wound dressing products: a translational investigation from the bench to the market. *Eng Regen*. 2022;3(2):182–200.
42. Moher D, Liberati A, Tetzlaff J, Altman DG. Preferred reporting items for systematic reviews and meta-analyses: the PRISMA statement. *PLoS Med*. 2009;6(7):e1000097. doi:10.1371/journal.pmed.1000097
43. Zmejkoski DZ, Marković ZM, Mitić DD, et al. Antibacterial composite hydrogels of graphene quantum dots and bacterial cellulose accelerate wound healing. *J Biomed Mater Res Part B Appl Biomater*. 2022;110(8):1796–1805. doi:10.1002/jbm.b.35037
44. Cheng C, Zhong H, Zhang Y, et al. Bacterial responsive hydrogels based on quaternized chitosan and GQDs-ε-PL for chemo-photothermal synergistic anti-infection in diabetic wounds. *Int J Biol Macromol*. 2022;210:377–393. doi:10.1016/j.ijbiomac.2022.05.008
45. Chekini M, Krivoshapkina E, Shkodenko L, et al. Nanocolloidal hydrogel with sensing and antibacterial activities governed by iron ion sequestration. *Chem Mater*. 2020;32(23):10066–10075. doi:10.1021/acs.chemmater.0c03362
46. Zhu Y, Lin L, Xie Y, et al. In situ self-assembly of polydopamine inside injectable hydrogels: antibacterial activity and photothermal therapy for superbug-infected wound healing. *Biomater Sci*. 2022;10(15):4126–4139. doi:10.1039/D2BM00310D
47. Shafique M, Sohail M, Minhas MU, et al. Bio-functional hydrogel membranes loaded with chitosan nanoparticles for accelerated wound healing. *Int J Biol Macromol*. 2021;170:207–221. doi:10.1016/j.ijbiomac.2020.12.157
48. Zmejkoski DZ, Zdravković NM, Trišić DD, et al. Chronic wound dressings – pathogenic bacteria anti-biofilm treatment with bacterial cellulose-chitosan polymer or bacterial cellulose-chitosan dots composite hydrogels. *Int J Biol Macromol*. 2021;191:315–323. doi:10.1016/j.ijbiomac.2021.09.118
49. Zmejkoski DZ, Marković ZM, Budimir MD, et al. Photoactive and antioxidant nanochitosan dots/biocellulose hydrogels for wound healing treatment. *Mater Sci Eng C*. 2021;122(111925):1–11. doi:10.1016/j.msec.2021.111925
50. Fiorica C, Palumbo FS, Pitarresi G, et al. Ciprofloxacin releasing gellan gum/polydopamine based hydrogels with near infrared activated photothermal properties. *Int J Pharm*. 2021;610(121131):1–9. doi:10.1016/j.ijpharm.2021.121231
51. Oliveira DML, Rezende PS, Barbosa TC, et al. Double membrane based on lidocaine-coated polymyxin-alginate nanoparticles for wound healing: in vitro characterization and in vivo tissue repair. *Int J Pharm*. 2020;591(120001):1–15. doi:10.1016/j.ijpharm.2020.120001
52. Günday C, Anand S, Gencer HB, et al. Ciprofloxacin-loaded polymeric nanoparticles incorporated electrospun fibers for drug delivery in tissue engineering applications. *Drug Deliv Transl Res*. 2020;10(3):706–720. doi:10.1007/s13346-020-00736-1
53. Wunnoo S, Lorenzo-Leal AC, Voravuthikunchai SP, Bach H. Advanced biomaterial agent from chitosan/ poloxamer 407-based thermosensitive hydrogen containing biosynthesized silver nanoparticles using Eucalyptus camaldulensis leaf extract. *PLoS One*. 2023;18(10):e0291505. doi:10.1371/journal.pone.0291505
54. Liang M, Dong L, Guo Z, et al. Collagen-hyaluronic acid composite hydrogels with applications for chronic diabetic wound repair. *ACS Biomater Sci Eng*. 2023;9(9):5376–5388. doi:10.1021/acsbiomaterials.3c00695
55. Sumini M, Souza de CR, Andrade GJS, et al. Cellulose hydrogel with hyaluronic acid and silver nanoparticles: sustained-release formulation with antibacterial properties against pseudomonas aeruginosa. *Antibiotics*. 2023;12(873):1–17. doi:10.3390/antibiotics12050873
56. Remaggi G, Bergamonti L, Graiff C, Ossiprandi MC, Elviri L. Rapid Prototyping of 3D-Printed AgNPs- and Nano-TiO2-Embedded hydrogels as novel devices with multiresponsive antimicrobial capability in wound healing. *Antibiotics*. 2023;12(1104):1–17. doi:10.3390/antibiotics12071104
57. Khalil AM, Hashem AH, Kamel S. Bimetallic hydrogels based on chitosan and carrageenan as promising materials for biological applications. *Biotechnol J*. 2023;18(2300093):1–11. doi:10.1002/biot.202300093
58. Barrett JP, Raby E, Wood F, et al. An in vitro study into the antimicrobial and cytotoxic effect of Acticoat^{TM} dressings supplemented with chlorhexidine. *Burns*. 2022;48(4):941–951. doi:10.1016/j.burns.2021.09.019

59. Harandi FN, Khorasani AC, Shojaosadati SA, Hashemi-Najafabadi S. Surface modification of electrospun wound dressing material by Fe2O3 nanoparticles incorporating Lactobacillus strains for enhanced antimicrobial and antibiofilm activity. *Surf Interfaces*. 2022;28(101592):1–14. doi:10.1016/j.surfin.2021.101592
60. Hezari S, Olad A, Dilmaghani A. Modified gelatin/iron- based metal-organic framework nanocomposite hydrogel as wound dressing: synthesis, antibacterial activity, and Camellia sinensis release. *Int J Biol Macromol*. 2022;218:488–505. doi:10.1016/j.ijbiomac.2022.07.150
61. de Oliveira DM, Menezes DB, Andrade LR, et al. Silver nanoparticles obtained from Brazilian pepper extracts with synergistic anti-microbial effect: production, characterization, hydrogel formulation, cell viability, and in vitro efficacy. *Pharm Dev Technol*. 2021;26(5):539–548. doi:10.1080/10837450.2021.1898634
62. Choudhary M, Chhabra P, Tyagi A, Singh H. Scar free healing of full thickness diabetic wounds: a unique combination of silver nanoparticles as antimicrobial agent, calcium alginate nanoparticles as hemostatic agent, fresh blood as nutrient/growth factor supplier and chitosan as base matrix. *Int J Biol Macromol*. 2021;178:41–52. doi:10.1016/j.ijbiomac.2021.02.133
63. Harandi FN, Khorasani AC, Shojaosadati SA, Hashemi-Najafabadi S. Living Lactobacillus–ZnO nanoparticles hybrids as antimicrobial and antibiofilm coatings for wound dressing application. *Mater Sci Eng C*. 2021;130(112457):1–15. doi:10.1016/j.msec.2021.112457
64. Bagheri M, Validi M, Gholipour A, Makvandi P, Sharifi E. Chitosan nanofiber biocomposites for potential wound healing applications: antioxidant activity with synergic antibacterial effect. *Bioeng Transl Med*. 2022;7(1):1–15. doi:10.1002/btm2.10254
65. Hasanin M, Swielam EM, Atwa NA, Agwa MM. Novel design of bandages using cotton pads, doped with chitosan, glycogen and ZnO nanoparticles, having enhanced antimicrobial and wounds healing effects. *Int J Biol Macromol*. 2022;197:121–130. doi:10.1016/j.ijbiomac.2021.12.106
66. Nozari M, Gholizadeh M, Zahiri Oghani F, Tahvildari K. Studies on novel chitosan/alginate and chitosan/bentonite flexible films incorporated with ZnO nano particles for accelerating dermal burn healing: in vivo and in vitro evaluation. *Int J Biol Macromol*. 2021;184:235–249. doi:10.1016/j.ijbiomac.2021.06.066
67. Zamani K, Allah-Bakhshi N, Akhavan F, et al. Antibacterial effect of cerium oxide nanoparticle against Pseudomonas aeruginosa. *BMC Biotechnol*. 2021;21(1):1–11. doi:10.1186/s12896-021-00727-1
68. Eivazzadeh-Keihan R, Khalili F, Khosropour N, et al. Hybrid bionanocomposite containing magnesium hydroxide nanoparticles embedded in a carboxymethyl cellulose hydrogel plus silk fibroin as a scaffold for wound dressing applications. *ACS Appl Mater Interfaces*. 2021;13 (29):33840–33849. doi:10.1021/acsami.1c07285
69. Targhi AA, Moammeri A, Jamshidifar E, et al. Synergistic effect of curcumin-Cu and curcumin-Ag nanoparticle loaded niosome: enhanced antibacterial and anti-biofilm activities. *Bioorg Chem*. 2021;115(105116):1–13. doi:10.1016/j.bioorg.2021.105116
70. Selvaraj S, Karuppaiah A, Karthik S, Sankar V. Synthesis and toxicity assessment of copper-based nano composite cream: an approach to enhance the antibacterial effect of mafenide acetate. *Inorg Nano-Metal Chem*. 2021;51(1):27–37. doi:10.1080/24701556.2020.1750428
71. Niranjan R, Kaushik M, Selvi RT, et al. PVA/SA/TiO2-CUR patch for enhanced wound healing application: in vitro and in vivo analysis. *Int J Biol Macromol*. 2019;138:704–717. doi:10.1016/j.ijbiomac.2019.07.125
72. Mahmoud NN, Hikmat S, Abu Ghith D, et al. Gold nanoparticles loaded into polymeric hydrogel for wound healing in rats: effect of nanoparticles' shape and surface modification. *Int J Pharm*. 2019;565:174–186. doi:10.1016/j.ijpharm.2019.04.079
73. Brandenburg KS, Calderon DF, Kierski PR, et al. Inhibition of Pseudomonas aeruginosa biofilm formation on wound dressings. *Wound Repair Regen*. 2015;23(6):842–854. doi:10.1111/wrr.12365
74. Tolker-Nielsen T. Pseudomonas aeruginosa biofilm infections: from molecular biofilm biology to new treatment possibilities. *Apmis*. 2014;122 (Suppl 138):1–51. doi:10.1111/apm.12335
75. Rybtke M, Hultqvist LD, Givskov M, Tolker-Nielsen T. Pseudomonas aeruginosa biofilm infections: community structure, antimicrobial tolerance and immune response. *J Mol Biol*. 2015;427(23):3628–3645. doi:10.1016/j.jmb.2015.08.016
76. Henna TK, Pramod K. Graphene quantum dots redefine nanobiomedicine. *Mater Sci Eng C*. 2020;110(110651):1–21. doi:10.1016/j.msec.2020.110651
77. Hajishoreh NK, Jamalpoor Z, Rasouli R, Asl AN, Sheervalilou R, Akbarzadeh A. The recent development of carbon-based nanoparticles as a novel approach to skin tissue care and management - A review. *Exp Cell Res*. 2023;433(113821):1–11. doi:10.1016/j.yexcr.2023.113821
78. Dong X, Liang W, Meziani MJ, Sun YP, Yang L. Carbon dots as potent antimicrobial agents. *Theranostics*. 2020;10(2):671–686. doi:10.7150/thno.39863
79. Hernández-Hernández AA, Aguirre-álvarez G, Cariño-Cortés R, Mendoza-Huizar LH, Jiménez-Alvarado R. Iron oxide nanoparticles: synthesis, functionalization, and applications in diagnosis and treatment of cancer. *Chem Pap*. 2020;74(11):3809–3824. doi:10.1007/s11696-020-01229-8
80. Gudkov SV, Burmistrov DE, Serov DA, Rebezov MB, Semenova AA, Lisitsyn AB. Do iron oxide nanoparticles have significant antibacterial properties? *Antibiotics*. 2021;10(7):1–23. doi:10.3390/antibiotics10070884
81. Liu J, Wu D, Zhu N, Wu Y, Li G. Antibacterial mechanisms and applications of metal-organic frameworks and their derived nanomaterials. *Trends Food Sci Technol*. 2021;109:413–434. doi:10.1016/j.tifs.2021.01.012
82. Bhardwaj N, Pandey SK, Mehta J, Bhardwaj SK, Kim KH, Deep A. Bioactive nano-metal-organic frameworks as antimicrobials against Gram-positive and Gram-negative bacteria. *Toxicol Res (Camb)*. 2018;7(5):931–941. doi:10.1039/C8TX00087E
83. Sirelkhatim A, Mahmud S, Seeni A, et al. Review on zinc oxide nanoparticles: antibacterial activity and toxicity mechanism. *Nano-Micro Lett*. 2015;7(3):219–242. doi:10.1007/s40820-015-0040-x
84. Zhang M, Zhang C, Zhai X, Luo F, Du Y, Yan C. Antibacterial mechanism and activity of cerium oxide nanoparticles. *Sci China Mater*. 2019;62 (11):1727–1739. doi:10.1007/s40843-019-9471-7
85. Pop OL, Mesaros A, Vodnar DC, et al. Cerium oxide nanoparticles and their efficient antibacterial application in vitro against gram-positive and gram-negative pathogens. *Nanomaterials*. 2020;10(8):1–15. doi:10.3390/nano10081614
86. Younis AB, Haddad Y, Kosaristanova L, Smerkova K. Titanium dioxide nanoparticles: recent progress in antimicrobial applications. *Wiley Interdiscip Rev Nanomed Nanobiotechnol*. 2023;15(3):1–25. doi:10.1002/wnan.1860
87. Halbus AF, Horozov TS, Paunov VN. Controlling the antimicrobial action of surface modified magnesium hydroxide nanoparticles. *Biomimetics*. 2019;4(41):1–20. doi:10.3390/biomimetics4020041
88. Dong C, Cairney J, Sun Q, Maddan OL, He G, Deng Y. Investigation of Mg(OH)2 nanoparticles as an antibacterial agent. *J Nanopart Res*. 2010;12(6):2101–2109. doi:10.1007/s11051-009-9769-9

89. Sánchez-López E, Gomes D, Esteruelas G, et al. Metal-based nanoparticles as antimicrobial agents: an overview. *Nanomaterials*. 2020;10(2):1–39. doi:10.3390/nano10020292
90. Mathur A, Parihar AS, Modi S, Kalra A. Photodynamic therapy for ESKAPE pathogens: an emerging approach to combat antimicrobial resistance (AMR). *Microb Pathog*. 2023;183(106307):1–8. doi:10.1016/j.micpath.2023.106307
91. Manivasagan P, Khan F, Hoang G, et al. Thiol chitosan-wrapped gold nanoshells for near-infrared laser-induced photothermal destruction of antibiotic-resistant bacteria. *Carbohydr Polym*. 2019;225(115228):1–11. doi:10.1016/j.carbpol.2019.115228
92. He X, Qian Y, Wu C, et al. Entropy-mediated high-entropy mxenes nanotherapeutics: NIR-II-enhanced intrinsic oxidase mimic activity to combat methicillin-resistant staphylococcus aureus infection. *Adv Mater*. 2023;35(26):1–17.
93. Ye L, He X, Obeng E, et al. The CuO and AgO co-modified ZnO nanocomposites for promoting wound healing in Staphylococcus aureus infection. *Mater Today Bio*. 2023;18(100552):1–13.
94. Lv J, Li B, Luo T, et al. Selective photothermal therapy based on lipopolysaccharide aptamer functionalized MoS2 nanosheet-coated gold nanorods for multidrug-resistant pseudomonas aeruginosa infection. *Adv Healthc Mater*. 2023;12(15):1–14.
95. Medaglia S, Otri I, Bernardos A, et al. Synergistic antimicrobial photodynamic therapy using gated mesoporous silica nanoparticles containing curcumin and polymyxin B. *Int J Pharm*. 2024;654(123947):1–12. doi:10.1016/j.ijpharm.2024.123947
96. Mirzahosseinipour M, Khorsandi K, Hosseinzadeh R, Ghazaeian M, Shahidi FK. Antimicrobial photodynamic and wound healing activity of curcumin encapsulated in silica nanoparticles. *Photodiagnosis Photodyn Ther*. 2020;29(101639):1–7. doi:10.1016/j.pdpdt.2019.101639
97. Azimzadeh M, Greco G, Farmani A, et al. Synergistic effects of nano curcumin mediated photodynamic inactivation and nano-silver@colistin against Pseudomonas aeruginosa biofilms. *Photodiagnosis Photodyn Ther*. 2024;45(103971):1–11. doi:10.1016/j.pdpdt.2024.103971
98. Ghasemi M, Khorsandi K, Kianmehr Z. Photodynamic inactivation with curcumin and silver nanoparticles hinders Pseudomonas aeruginosa planktonic and biofilm formation: evaluation of glutathione peroxidase activity and ROS production. *World J Microbiol Biotechnol*. 2021;37(9):1–10. doi:10.1007/s11274-021-03104-4
99. Mushtaq S, Yasin T, Saleem M, Dai T, Yameen MA. Potentiation of antimicrobial photodynamic therapy by curcumin-loaded graphene quantum dots. *Photochem Photobiol*. 2022;98(1):202–210. doi:10.1111/php.13503
100. Parasuraman P, Thamanna RY, Shaji C, et al. Biogenic silver nanoparticles decorated with methylene blue potentiated the photodynamic inactivation of Pseudomonas aeruginosa and Staphylococcus aureus. *Pharmaceutics*. 2020;12(8):1–18. doi:10.3390/pharmaceutics12080709
101. Rocca DM, Silvero CMJ, Aiassa V, Cecilia Becerra M. Rapid and effective photodynamic treatment of biofilm infections using low doses of amoxicillin-coated gold nanoparticles. *Photodiagnosis Photodyn Ther*. 2020;31(101811):1–7. doi:10.1016/j.pdpdt.2020.101811
102. Prema D, Binu NM, Prakash J, Venkatasubbu GD. Photo induced mechanistic activity of GO/Zn(Cu)O nanocomposite against infectious pathogens: potential application in wound healing. *Photodiagnosis Photodyn Ther*. 2021;34(102291):1–23. doi:10.1016/j.pdpdt.2021.102291
103. Garin C, Alejo T, Perez-Laguna V, et al. Chalcogenide nanoparticles and organic photosensitizers for synergetic antimicrobial photodynamic therapy. *J Mater Chem B*. 2021;9(31):6246–6259. doi:10.1039/D1TB00972A
104. Mo S, Zhao Y, Wen J, et al. Efficient photothermal and photodynamic synergistic antibacterial therapy of Cu7S4 nanosheets regulated by facet engineering. *J Hazard Mater*. 2022;432(128662):1–11. doi:10.1016/j.jhazmat.2022.128662
105. He X, Lv Y, Lin Y, et al. Platinum nanoparticles regulated V2C MXene Nanoplatforms with NIR-II enhanced nanozyme effect for photothermal and chemodynamic anti-infective therapy. *Adv Mater*. 2024;2400366:1–17.
106. Liu Z, Liu Z, Zhao Z, et al. Photothermal Regulated nanozyme of cufes2 nanoparticles for efficiently promoting wound healing infected by multidrug resistant bacteria. *Nanomaterials*. 2022;12(2469):1–16.
107. Dai X, Ma J, Chen N, et al. MSNs-Based Nanocomposite for Biofilm Imaging and NIR-Activated Chem/Photothermal/Photodynamic Combination Therapy. *ACS Appl Bio Mater*. 2021;4(3):2810–2820. doi:10.1021/acsabm.1c00034
108. Zielińska A, Carreiró F, Oliveira AM, et al. Polymeric Nanoparticles: production, Characterization, Toxicology and Ecotoxicology. *Molecules*. 2020;25:1–20.
109. Shariati A, Chegini Z, Ghaznavi-Rad E, Zare EN, Hosseini SM. PLGA-Based Nanoplatforms in Drug Delivery for Inhibition and Destruction of Microbial Biofilm. *Front Cell Infect Microbiol*. 2022;12(926363):1–18. doi:10.3389/fcimb.2022.926363
110. Rashki S, Asgarpour K, Tarrahimofrad H, et al. Chitosan-based nanoparticles against bacterial infections. *Carbohydr Polym*. 2021;251(117108):1–12. doi:10.1016/j.carbpol.2020.117108
111. Severino P, Da silva CF, Andrade LN, de Lima Oliveira D, Campos J, Souto EB. Alginate Nanoparticles for Drug Delivery and Targeting. *Curr Pharm Des*. 2019;25(11):1312–1334. doi:10.2174/1381612825666190425163424
112. Tang Y, Tan Y, Lin K, Zhu M. Research Progress on Polydopamine Nanoparticles for Tissue Engineering. *Front Chem*. 2021;9(727123):1–9. doi:10.3389/fchem.2021.727123